HHS Public Access

Author manuscript

J Med Chem. Author manuscript; available in PMC 2024 May 25.

Published in final edited form as:

J Med Chem. 2023 May 25; 66(10): 6523–6541. doi:10.1021/acs.jmedchem.3c00034.

Fragment-based approaches to identify RNA binders

Blessy M. Suresh,
UF Scripps Biomedical Research & The Scripps Research Institute, Department of Chemistry, 130 Scripps Way, Jupiter, Florida 33458, United States

Amirhossein Taghavi,
UF Scripps Biomedical Research & The Scripps Research Institute, Department of Chemistry, 130 Scripps Way, Jupiter, Florida 33458, United States

Jessica L. Childs-Disney,
UF Scripps Biomedical Research & The Scripps Research Institute, Department of Chemistry, 130 Scripps Way, Jupiter, Florida 33458, United States

Matthew D. Disney*
UF Scripps Biomedical Research & The Scripps Research Institute, Department of Chemistry, 130 Scripps Way, Jupiter, Florida 33458, United States

Abstract

Although fragment-based drug discovery (FBDD) has been successfully implemented and well-explored for protein targets, its feasibility for RNA targets is emerging. Despite the challenges associated with the selective targeting of RNA, efforts to integrate known methods of RNA binder discovery with fragment-based approaches have been fruitful, as a few bioactive ligands have been identified. Here, we review various fragment-based approaches implemented for RNA targets and provide insights into experimental design and outcomes to guide future work in the area. Indeed, investigations surrounding the molecular recognition of RNA by fragments address rather important questions such as the limits of molecular weight that confer selective binding and the physicochemical properties favorable for RNA binding and bioactivity.

Graphical Abstract

*Corresponding Author Author to whom correspondence should be addressed: Disney@scripps.edu.

The authors declare the following competing financial interest(s): M.D.D. is a founder of Expansion Therapeutics.

Supporting Information

The Supporting Information is available free of charge at https://pubs.acs.org/doi/10.1021/acs.jmedchem.3c00034.

Table S1, which reports the physicochemical properties of the fragments described herein (PDF)

jm3c00034_si_001.pdf (143.58 kb)

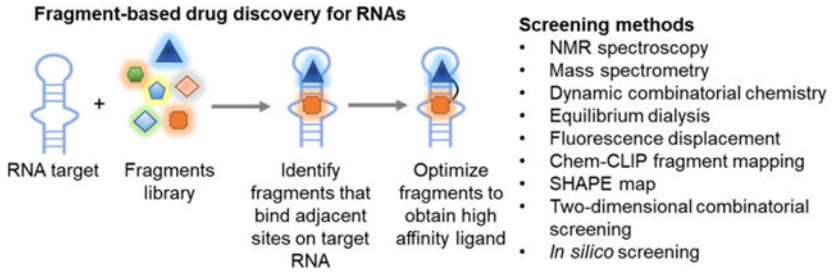

INTRODUCTION

The Encyclopedia of DNA Elements (ENCODE) Project showed that only ~1–2% of the human genome encodes for protein, yet ~75% is transcribed into RNA. (9) Functional studies have elucidated that noncoding (nc)RNAs can be subdivided into multiple classes (*i.e.,* long noncoding (lnc)RNAs, micro (mi)RNAs, small nuclear (sn)RNAs, etc.) that exhibit regulatory functions critical for proper cellular functioning. (10−12) Therefore, it is not surprising that the dysregulation of these ncRNAs is causative of or associated with diseases, including cancer, hepatitis C viral infections, cardiovascular disease, atherosclerosis, and diabetes, among many others. (15−18) Therefore, targeting RNAs opens up a large therapeutic space that can be explored with small molecules.

Targeting RNAs using antisense oligonucleotides (ASOs), where the short oligonucleotide forms Watson–Crick base pairing with the target RNA, has been an invaluable tool in studying and affecting RNA function. (25) The ASO base pairs with target RNA and either sterically blocks RNA–RNA or RNA–protein interactions or promotes degradation of RNA via an RNase H mediated pathway. (25) This method has been successful with FDA-approved ASOs available; however, there are challenges associated with nonspecificity, efficacy, and limited delivery. (26) An alternative to ASOs is targeting structured regions of RNA using small molecules. Small molecules can be optimized to overcome some of the challenges associated with ASOs, for example favorable pharmacodynamic and pharmacokinetic profiles, traditional medicinal chemistry approaches can be employed. (27) While ASOs can be easily designed to target unstructured regions of RNA, (28) small molecules target structured regions, and thus the two approaches are complementary, increasing the druggable RNA space.

RNA sequences fold into distinct three-dimensional structures, yielding small-molecule-targetable structural motifs including internal loops, bulges, hairpins, pseudoknots, and quadruplexes. (29) That is, the three-dimensional structure of RNA is an ensemble of the local structural elements which can be targeted using small molecules. First examples of small molecules targeting these structural elements and affecting function came from ribosomes and riboswitches. Aminoglycoside binders target the ribosomal A-site and are antibactericidal, (30) while small molecules mimicking the native ligand for riboswitches were identified demonstrating functional activity. (31,32) Following these reports many small molecules, targeting a wide variety of disease relevant RNAs, including repeat expansions, (33) microRNAs, (34) mRNAs, (35) etc., have been reported. (36)

An approach that could help accelerate small molecule discovery for RNA targets is fragment-based drug discovery (FBDD). In this approach, small fragments, typically less than 300 Da molecular weight with less than three hydrogen bond donors/acceptors and a ClogP (partition coefficient) value less than 3, (37) are screened for specific binding to an RNA target of interest (Figure 1). These fragments can then be optimized to enhance affinity and selectivity by (i) merging scaffolds that bind overlapping regions on the target (fragment merging); (ii) linking two fragments together that bind adjacent sites in the target (fragment linking); or (iii) adding functional groups that interact with the target (fragment growing) (Figure 1). (7) The optimized ligand is expected to have increased affinity owing to the thermodynamic parameters of binding two fragments. (38) That is, the combined ligand gives more than an additive increase in binding energy compared to individual fragments. (39,40) For example, in the case of linking two fragments, the energy of binding of the assembled ligand (ΔG_{AB}) is the sum of binding energies of individual ligands (ΔG_A and ΔG_B) plus a Gibbs free energy term associated with linking, or connection Gibbs energy (ΔG^S). (24) ΔG^S is largely an entropic term corresponding to translational and rotational entropy, conformational changes of the target upon binding, and strain or destabilization associated with the binding event (Figure 1). (38) Assuming that the enthalpic parameters are favorable, the entropy cost of binding one linked molecule is less than the entropy cost of binding two separate fragments (linking coefficient, $E < 1$). (38,41) This can yield a linked molecule with an affinity greater than the combined affinities of the individual fragments (Figure 1). (24) However, such favorable linking conditions are difficult to achieve and are therefore rare. Despite that, even with $E > 1$, high-affinity interactions capable of producing a bioactive interaction can be achieved by linking two fragments, which has been widely explored in the protein FBDD field. (42)

Fesik et al. reported “SAR by NMR” in 1996, now considered a seminal paper in the field of FBDD. Nuclear magnetic resonance (NMR) spectroscopy was used to screen low molecular weight fragments, followed by linking of fragments that bind to adjacent sites to obtain a low nanomolar binder of FK506 binding protein (FKBP). (43) Since then, this approach has been used to generate novel ligands for proteins, (44,45) leading to FDA approved drugs—ABT-199, (46) Vemurafenib, (47) Asciminib, (48) Erdafitinib, (49) Pexidartinib, (50) Sotorasib, (51) and Venetoclax (52)—as well as several compounds in clinical trials. (53)

FBDD has not been widely applied to RNA targets due to the challenges posed by the rarity of hydrophobic pockets and its high conformational flexibility, although such an approach could be advantageous, as only 10–14% of proteins have active binding sites that can be targeted with small molecules. (54,55) One of the major areas of development for small molecule targeting of RNAs is identification of new chemical scaffolds. Since traditional small molecule targeting approaches were directed toward protein targets, there is a dearth of information describing the chemical space that has preferential binding to RNA, *i.e.*, the current commercially available compound libraries are likely biased for protein binding. Therefore, the design of compound libraries with diverse chemical scaffolds and screening of these libraries against a variety of RNA targets are needed to generate chemical space with selective affinity for RNA targets. (36) Fragment-based approaches are particularly attractive in this regard, as fragments can cover a large, diverse chemical space using

a fewer number of compounds compared to traditional compound libraries. (56) Major challenges in fragment-based screening for RNA targets are the detection of low-affinity binding fragments (high μM to mM range) and their short residence times. (44,45,57−60) Here, we describe various strategies adopted to study fragments that bind RNA and the optimization thereof.

Fragment-Based Approaches in RNA

Identifying fragments that bind RNAs is more challenging than identifying proteins, as RNAs have highly flexible structures and lack hydrophobic pockets that can be easily targeted. Therefore, FBDD for RNA targets must integrate structural studies and innovative screening strategies to enable the detection of low-affinity fragment–RNA interactions. That is, structural information about the fragments in complex with RNA informs optimization to improve the affinity and selectivity of individual fragments and also informs how to link two or more fragments together. (14) Indeed, novel strategies to identify fragments that bind RNAs and the optimization thereof have been developed by various laboratories, (61) employing NMR spectroscopy, (3,4,21) mass spectrometry, (21,62) dynamic combinatorial chemistry (DCC), (19) equilibrium dialysis, (8) labeled ligand displacement methods, chemical cross-linking and isolation by pull-down (Chem CLIP), (5,23) selective 2′-hydroxyl acylation analyzed by primer extension and mutational profiling (SHAPE-MaP), (2,22) two-dimensional combinatorial screening (2DCS), (22) and *in silico* methods. (14) Here, we describe the above-mentioned biophysical strategies employed to identify fragment binders with one detailed example for each methodology.

Nuclear Magnetic Resonance (NMR) Spectroscopy

NMR spectroscopy has proven to be an invaluable technique in FBDD, (63−65) particularly to discriminate binders from nonbinders in a mixture of compounds, (66) enabling efficient exploration of diverse chemotypes. Further, NMR spectroscopy is able to detect binding affinities in the μM to mM range, ideal for fragments. (67−69) Multiple techniques have been developed to detect ligand binding using NMR spectroscopy, including: (i) T_2-filter, (70) (ii) paramagnetic NMR, (71) (iii) saturation transfer difference (STD), (72,73) (iv) water-ligand observed via gradient spectroscopy (WaterLOGSY), (74) and (v) fluorine chemical shift anisotropy and exchange for screening (FAXS; for ^{19}F-containing molecules). (75,76) The following case studies describe how these NMR spectroscopy techniques were implemented for fragment-based ligand discovery for RNAs.

i. One-Dimensional (1D) NMR Spectroscopy—1D NMR spectroscopy can be applied effectively to detect structural changes of RNA upon binding to low molecular weight compounds. (77) These structural rearrangements result in changes in chemical shifts or line broadening of the imino peaks that are easily detectable in 1D NMR spectra.

In one example, to identify fragments that bind the influenza A virus promoter (RNA), a library of 4,279 small molecular weight fragments was screened by looking for changes in the 1D imino proton spectrum of the RNA, whether line broadening or changes in chemical shift (Figure 2A). (3) Seven fragments were identified as initial hits; among them, compound **1** induced the most drastic changes in the 1D NMR spectra (Figure

2A). The binding affinity of **1** was measured by recording 1D NMR spectra at various concentrations of compound, affording a K_d of 50 ± 9 μM. The structure of the viral promoter-**1** complex was elucidated using nuclear Overhauser effect spectroscopy (NOESY) combined with residual dipolar coupling (RDC) data and X-PLOR (structure determination by using minimization protocols based on molecular dynamics (MD) approaches). (78−80) Interestingly, **1** inhibited replication of both influenza A and B viruses with EC_{50} values in the range of 71–275 μM as well as viral plaque formation. (3) Although not as high throughput as other methods described herein, this case study demonstrates the power of NMR spectroscopy as a robust method to measure fragment binding from initial hit identification to structure determination.

ii. ^{19}F 1D NMR Spectroscopy—^{19}F NMR spectroscopy has several advantages compared to ^{1}H, including a higher chemical shift dispersion (83 vs 10 ppm, respectively) and single resonance frequency of each ^{19}F, which makes the observation of multiple fragments in a mixture possible. In one study, ^{19}F NMR spectroscopy was employed to screen 101 fragments against 14 different RNA structures to evaluate their druggability. (4) RNA hairpins, bulges, internal loops, pseudoknots, and riboswitches comprised the RNA screening pool. Initial screening, completed in batches of ~20 fragments, was conducted as ^{19}F transverse relaxation experiments, which apply Carr–Purcell–Meiboom–Gill (81) (CPMG) pulse trains to measure the different relaxation times of target-bound vs unbound fragments. The fragment library was also counter screened against five transfer (t)RNAs, five DNA oligonucleotides, and five protein targets to eliminate nonspecific binders. Overall, the highest hit rates were observed for protein targets, followed by RNA and DNA.

The fragments that bound were further investigated by 2D NMR spectroscopy techniques (^{1}H and ^{15}N correlation experiments) and titration experiments to detect the changes in chemical shifts of the RNA's nucleotides after the addition of ligands. As a proof-of-concept, to study whether linking fragments can lead to an increase in binding affinity, one of the initial fragment hits, **2**, was linked to a known intercalator compound, acridine (**3**), to obtain compound **4** which targets a structure in the *S*-adenosylmethionine (SAM) riboswitch antiterminator (Figure 2B). Compound **4** showed an increase in binding affinity (K_d = 1 μM) when compared to that of the starting fragment (**3**, K_d = 59 μM) (Figure 2B). This study shows the usefulness of ^{19}F NMR spectroscopy in fragment hit identification.

iii. T_2 Relaxation NMR Spectroscopy—Although STD spectroscopy is a useful method for fragments that bind proteins, low proton density within nucleobases of RNA (or generally in nucleic acids) impedes the effective magnetization transfer from the macromolecule to the bound fragment. (82) As an alternative, the T_2 approach has been developed, (83) which assumes that small molecules, upon binding to RNA, adopt the relaxation time of the RNA–ligand complex. By measuring the transverse relaxation rates in the absence and presence of RNA, binding vs nonbinding fragments can be distinguished.

This method was applied to screen 1,000 fragments, in batches of 9–11 compounds, against a model of the *Myocbacterium tuberculosis* peptidyl transferase center (PTC) present in the bacteria's ribosomal (r)RNA (Figure 2C). (21) Nine fragments were selected with the largest changes in T_2, four of which contained a phenylthiazole moiety. (21) The ZINC database

with 230 million compounds was then queried for molecules containing the phenylthiazole moiety, yielding 919 molecules that were docked against the ribosomal PTC crystal structure and consequently ranked based on their binding affinity. Finally, machine learning was used to study structure–activity relationships, and the ten molecules with the best docking free energy scores were selected for further study. They were then evaluated in an *in vitro* transcription–translation assay, where compounds **5** and **6** inhibited translation with IC_{50} values of 9.1 and 2.8 μM, respectively (Figure 2C). Collectively, this study showed the power of integrating multiple strategies for fragment-based discovery using T_2 relaxation NMR spectroscopy, docking, and machine learning.

iv. WaterLOGSY—WaterLOGSY is based on the magnetization transfer from bulk water to the RNA and then to a bound ligand. (84) It is a sensitive technique especially for detecting low-affinity binding compounds like fragments (Figure 3A). (74) Spin diffusion, facilitated by the residence times of water molecules in the binding pockets (ranging from ns to hundreds of μs), can also occur between water molecules and protons on heteroatoms in the RNA. This residence time is longer than the time (300 ps) required to observe intermolecular water–RNA NOEs. As a result of these time differences, NOEs between water and the ligand, binding vs nonbinding, can be distinguished. Binding ligands interact with proton spins of inverted water with negative cross-relaxation rates, whereas nonbinding ligands have positive cross-relaxation rates. It should be noted that compounds with exchangeable protons will give strong WaterLOGSY signals, while those that do not contain exchangeable protons will have poor or no signals. Further, WaterLOGSY is only suitable for compounds that bind with K_d values in the μM to mM range; high-affinity compounds cannot be identified by WaterLOGSY. (84) In one example, WaterLOGSY and T_2 relaxation time spectroscopy were used to screen 102 fragments (3–4 compounds per sample) for binding to a 27-nucleotide model of the rRNA aminoacyl (A)-site, yielding five hit compounds (**7**–**11**; Figure 3B). (20) This screening yielded two new compounds (**10** and **11**) that were not previously identified as binders to the ribosomal A-site.

Mass Spectrometry

Electrospray ionization mass spectrometry (ESI-MS) has been used for the detection of low-affinity binding complexes between nucleic acids and small molecules. (85,86) In this approach, a high-resolution mass spectrometer, for example, a Fourier transform ion cyclotron resonance (FT-ICR) mass spectrometer, is employed to characterize complexes between an RNA and a ligand (Figure 4A). (87,88) After identifying binding molecules, affinity and stoichiometry can be measured in a high-throughput format by MS-MS. (89) Information about the binding site and binding mode—concurrent, competitive, or cooperative—can be identified as well, as the method can detect both free and complexed fractions of RNA. Importantly, binding site and binding mode data in concert with structure–activity relationship (SAR) studies can guide the linkage of two fragments into a single compound, increasing affinity and selectivity.

The first use of MS for RNA targets, dubbed “SAR by MS”, studied the binding of fragments to the 1061 nucleotide region of the bacterial 23S rRNA, an RNA element that binds ribosomal protein L11 and the binding site for the antibiotic thiostrepton (Figure

4B). (13) Here, the authors used a mutant RNA, U1061A, the structure of which was elucidated by X-ray crystallography. (90) The U1061A substitution stabilizes the proper fold of the 58-mer subdomain. SAR by MS identified two classes of small molecules that bound the mutant RNA: d-amino acids and quinoxalin-2,3-diones. With the goal of identifying derivatives of the d-amino acids and quinoxalin-2,3-diones that bind different sites, competitive MS experiments were carried out with derivatives of two classes of compounds. Since these classes are structurally different, it was hypothesized that they bind distinct sites within the RNA target. This hypothesis was validated by the competition experiment where derivatives showed concurrent (**12** and **13**, **14** and **15**) and cooperative (**12** and **15**) binding in the presence of the ternary complex.

Using the information from competitive studies, which also yielded SAR, a representative of each class, **15** and **16**, were linked together with different linker moieties. Their binding affinities and abilities to inhibit bacterial transcription/translation in a cell-free functional assay were then measured (Figure 4B). One of the assembled fragments, **17**, demonstrated improved binding affinity (K_d = 6.5 μM) and functional inhibition (IC_{50} = 14 μM) compared to those of the starting fragments (K_d > 100 μM, IC_{50} > 100 μM). (13) Although the assembled compounds inhibited translation *in vitro*, they had no antibacterial activity (Figure 4B). In a follow-up work, **17** was further optimized to afford the antibacterial **18**, which had a minimum inhibitory concentration (MIC) of 3–6 μM against *Staphylococcus aureus* and 6–13 μM against *Escherichia coli* (Figure 4B). (91)

SAR by MS also led to the discovery of a new class of RNA-binding small molecules for hepatitis C virus (HCV). (62) The IIA subdomain of HCV's internal ribosomal entry site (IRES) was screened against a 180,000-member compound library, which yielded benzimidazoles as a hit scaffold. SAR studies and a fragment growing strategy identified a compound with improved affinity (K_d = 0.7 μM vs >100 μM for starting benzimidazole hit) and activity in an HCV-replicon assay. (62)

Taken together, mass spectrometry has been successfully implemented to identify fragments that bind bacterial and viral RNAs that were subsequently optimized to obtain antibacterials and antivirals. We expect that such methods will be implemented for other types of RNAs in the near future and that more chemically diverse fragments will be studied.

Dynamic Combinatorial Chemistry (DCC)

Dynamic combinatorial chemistry (DCC) is a target-aided selection of high-affinity ligands achieved by equilibration of combinatorial libraries. First described for DNA targets in 2006, (92) DCC was later applied to RNA targets, particularly resin bound DCC (RB-DCC). (93,94) In RB-DCC, a library of building blocks is covalently attached to a solid support with disulfide functionality appended for a reversible reaction. The library is equilibrated with the same building blocks present as thiols in solution and the fluorescently labeled RNA target. As this is an equilibrium measurement, the resin bound building blocks can react with solution phase building blocks to yield dimers. After equilibration, the beads are imaged by fluorescence microscopy where fluorescence indicates binding of the target (Figure 5A).

In one example of RB-DCC, the frameshift regulatory structure from human immunodeficiency virus (HIV)-1 RNA was equilibrated with a solid phase and solution phase building block library (n = ~150), which afforded a library with theoretically 11,325 members. (19) Three beads were identified visually with the highest fluorescence (hit rate = 0.03%), yielding building block **19** as one of the three building block hits (Figure 5B). All potential combinations of the three monomer hits were synthesized into dimers, yielding nine in total. Dimers binding to the RNA target were then evaluated on the beads in a similar manner by using fluorescence microscopy. Two dimer beads had high fluorescence intensity visually; among the two, **20** was superior with an affinity of 4.1 ± 2.4 μM for the HIV-1 frameshift regulatory element, as compared to >90 μM for the other dimer. This binding was selective, as no measurable binding affinity or K_d > 90 μM was observed for the homologous DNA sequence and other RNA structures (an RNA hairpin from the *Pneumocystis carinii* group I intron, an RNA stem-loop with an altered loop sequence, and a short version of the HIV-1 frameshift regulatory element) (Figure 5B). (19) Optimization of **20** afforded **21**, which bound the target 250-fold more tightly (K_d = 16 nM) and inhibited the infectivity of pseudotyped HIV and live HIV virus (Figure 5B). (95,96)

The proof-of-concept studies described above demonstrated that RB-DCC can be used as a platform to study libraries of building blocks, in a combinatorial fashion, for binding to RNA. Indeed, following this study, targeting other RNA structures were also explored using RB-DCC. (97,98) However, most of the monomers identified as hits have molecular weights that render the assembled dimers bulky. Therefore, we foresee future work in the area focusing on expanding the chemical diversity of the building blocks, as well as reducing their molecular weights.

Equilibrium Dialysis

In equilibrium dialysis, a labeled ligand (or one that is inherently fluorescent) and the RNA target are placed in two chambers separated by a dialysis membrane. Once equilibrium is reached, the distribution of the labeled ligand between the two chambers is measured. If the study is conducted as a function of ligand concentration, a K_d can be measured. (99) In 2010, Abell and co-workers described a method for fragment screening using competitive equilibrium dialysis. (100) In this approach, the ability of a fragment to compete with a known ligand's binding to the RNA target was measured by calculating the differential distribution of the labeled ligand (Figure 6). Here, the known ligand, which is labeled, and the RNA are placed in one chamber and the candidate fragment is placed in the other. Once equilibrium is reached, the percentage of labeled ligand displaced from the RNA is measured, indicative of the fragment's affinity for the RNA target.

Abell and co-workers tested this approach for targeting the *E. coli ThiM* riboswitch. Riboswitches are conformational switches present in the transcriptome that are responsive to the binding of cellular metabolites, thereby regulating gene expression. They contain an aptamer domain, which, when bound to the target ligand, undergoes structural changes, triggering changes in the folding pattern of the expression platform, thereby regulating the gene expression. (101) The *ThiM* riboswitch senses the coenzyme thiamine pyrophosphate (TPP) and regulates the synthesis of proteins in its biosynthetic pathway (Figure 6A).

To identify fragments that bind the *ThiM* riboswitch, competition equilibrium dialysis was employed using [^{3}H] thiamine and a library of ~1,300 commercially available fragments. The fragments were screened in pools of five, affording hits in 32 of 252 mixtures. Binders were deconvoluted and validated via equilibrium dialysis, providing 20 fragments from 16 cocktails (hit rate = 2%). To eliminate the compounds that demonstrated nonspecific binding to RNA, a counterscreen employing the lysine-responsive *lysC* riboswitch was performed, affording 10 selective fragments (**22**–**25** are representative selective hits; Figure 6C). None of the fragments identified from the competitive equilibrium dialysis studies inhibited riboswitch activity in an *in vitro* assay, (8) suggesting that binding was not sufficient to induce structural changes or affect downstream gene expression. Subsequently, the structures of four fragments bound to the riboswitch were elucidated by X-ray crystallography and/or selective 2′-hydroxyl acylation analyzed by primer extension (SHAPE) mapping, which showed that fragments induce an alternative structure of the riboswitch upon binding as compared to the native ligand. (102)

Taken together, competitive equilibrium dialysis can indeed identify fragments that bind RNA targets with affinities in the μM to mM range and can be used in conjunction with other methods (NMR spectroscopy, isothermal titration calorimetry (ITC), X-ray crystallography, and SHAPE) to study fragment–RNA binding interactions. This method does not require chemical modification of the RNA or fragment; however, it does require availability of a labeled, known ligand for competitive screening.

Labeled Ligand Displacement Methods

Akin to competitive equilibrium dialysis, labeled ligand displacement identifies fragment hits by changes in fluorescence caused by the release of a fluorescently labeled known ligand. Transactivation response (TAR) element RNA is a ncRNA element present in the 5′ untranslated region (UTR) of the HIV-1 RNA genome and is essential for viral replication. A viral regulatory protein, Tat, binds this RNA element, and the resultant complex recruits a transcriptional elongation factor to enact gene expression. In 2014, Gobel and co-workers reported a labeled ligand displacement methodology to study binding of fragments to TAR RNA. (1) This method employed Tat peptide binder (103) appended with donor and acceptor dye to study binding of fragments to a 31-mer TAR RNA element construct with a UCU internal bulge (Figure 7A). (104) Upon binding of the RNA, the fluorescently labeled Tat peptide unfolds and produces a fluorescence resonance energy transfer (FRET) signal. If a molecule competes with the peptide, it refolds and FRET is reduced.

Initially seven fragment elements (including benzene rings for their ability to form stacking and hydrophobic interactions with RNA, amines, amidines, and guanidines for their ability to form hydrogen bonds in their protonated state under physiological conditions) were studied for binding via the fluorometric competition assay. However, none of them displaced the fluorescently labeled Tat peptide probe at biologically relevant concentrations (IC_{50} > 2 mM). Based on the initial results, fragment elements were grown by adding aromatic rings and ring closures to increase the planarity of the structures and the stacking surface, and their binding was studied using the same competition assay. Fusing guanidine with a second benzene ring gave compound **26** with improved affinity (IC_{50} = 50 μM; Figure 7B). The

structural features of two weak isoquinoline binders were combined to obtain compound **27** which also showed increased binding affinity (IC_{50} = 150 μM) compared to that of the individual fragments (Figure 7B). Similarly, structural features of isoquinoline and quinazoline were combined to obtain a compound with increased affinity (IC_{50} = 400 μM), and binding affinity was further improved by adding an amine group to obtain compound **28** (IC_{50} = 40 μM; Figure 7B). This study demonstrates rational optimization of fragments based on the binding affinities of individual fragments. However, the functional activity of the compounds is not reported. Although this method can identify fragments that bind an RNA target, it requires a known binder, which could limit its broad applicability.

Chemical Cross-Linking and Isolation by Pull-Down Fragment Mapping (Chem-CLIP-Frag-Map)

To overcome challenges associated with the low-affinity binding interactions between fragments and RNA as well as their short residence times, chemical cross-linking and isolation by pull-down-fragment mapping (Chem-CLIP-Frag-Map) was developed. (5) In this platform, fully functionalized fragments (FFFs), previously used in protein ligand discovery, (105) were employed. FFFs comprise a potential RNA-binding moiety appended with diazirine (a cross-linking module) and an alkyne handle (for the isolation of RNA–FFF complexes). Upon irradiation, binding fragments are cross-linked to a labeled RNA target; adducts are pulled down by clicking the alkyne handle to azide-functionalized beads or to biotin for subsequent incubation with streptavidin beads. Binding of FFF probes is quantified by measuring the amount of labeled RNA associated with the beads (Figure 8A).

As a proof-of-concept, 460 FFFs were screened for binding to the precursor of microRNA-21 (pre-miR-21), an oncogenic miRNA upregulated in various cancers. (106,107) Of the 460 fragments, 21 compounds bound pre-miR-21 and were subjected to a competitive Chem-CLIP (C-Chem-CLIP) experiment with a known binder, **29**. Compound **29** binds to the Dicer processing site of pre-miR-21 and inhibits its biogenesis, albeit at μM concentrations (IC_{50} = ~10 μM). (108) The hypothesis was that a fragment that binds adjacent to the Dicer site could be coupled to **29** to afford a higher affinity and more potent heterodimer. Three fragments (**30**–**32**) did not compete with **29**, indicating binding to a different site; one of the three (**32**) demonstrated cooperative binding with **29**. These three fragments were assembled with **29** with different linker lengths, and the optimal heterodimer was identified by using a competitive cleavage assay, yielding heterodimer **33** (Figure 8A). Importantly, conjugation of the low molecular weight fragment (121 Da) afforded a 60-fold increase in binding affinity compared to **29** (K_d of 352 nM vs 18 μM). Further, **33** inhibited miR-21's biogenesis in MDA-MB-231, triple negative breast cancer (TNBC) cells, with an IC_{50} of ~1 μM, de-repressed two of miR-21's direct targets, PTEN (phosphatase and tensin homologue) and PDCD4 (programmed cell death 4 protein), and reduced the invasiveness of the TNBC cells. Heterodimer **33** was also more selective than **29** in a miRnome-wide profiling experiment, where the effect of the compound on ~370 microRNAs expressed in MDA-MB-231 was measured. Overall, this proof-of-concept study described a new strategy to study binding of fragments to RNA and demonstrated that assembled fragments that bind two adjacent sites have increased affinity and selectivity for the RNA target.

A recent study demonstrated that the binding of FFFs can be studied transcriptome-wide; that is, they can be screened for binding to the RNA target agnostically (Figure 8B). (23) A panel of 34 FFFs was first studied for *in vitro* binding to total RNA extracted from MDA-MB-231 TNBC cells using Chem-CLIP. Here, after cross-linking, the alkyne handle was clicked to the fluorescent dye TAMRA, and bound RNAs were visualized after separation by gel electrophoresis. Of the 34 FFFs, six cross-linked to RNA.

MDA-MB-231 cells were treated with these six FFFs, followed by cross-linking and pull-down with azide-functionalized beads. The RNAs pulled down by each FFF were identified by RNA-seq analysis and compared with a control diazirine probe lacking a potential RNA-binding moiety. The resulting data were analyzed by Genrich (109) to afford a binding landscape for each FFF. Genrich is an RNA sequencing analysis tool that uses a null model with a log-normal distribution to calculate the statistical significance of enrichment of a region of transcript by comparing the RNA sample before and after pull-down. Of the six FFFs, **34** and **35** were the most selective, pulling down 51 and 35 transcripts, respectively (compared to >70 for the other four fragments). Fragment **34** also yielded the highest enrichment of transcripts observed, with two transcripts enriched >12-fold, quiescin sulfhydryl oxidase 1 (*QSOX1*) and sequestosome 1 (*SQSTM1*). Notably, **34** specifically bound RNA as it did not bind DNA or protein; that is, its entire interactome was studied.

As cross-linking events can reduce or inhibit the processivity of reverse transcriptase, the RNA-seq data were analyzed for “RT stops”, which informs the FFF binding site. Modeling of the structure adopted by *QSOX1* and *SQSTM1* using ScanFold (110) (a scanning window free energy minimization program that identifies regions of structure within an RNA that have unusual thermodynamic stability) showed that the binding site of **34** is a U bulge within a hairpin structure of *QSOX1*, while, for *SQSTM1*, the RT stop site was found in the hairpin loop region. *QSOX1* is an enzyme that is overexpressed in a variety of tumors (111,112) and has two isoforms, *QSOX1a* and *QSOX1b*. The predicted U-bulge binding site is present only in *QSOX1a*, suggesting that **34** could be isoform-specific. Fragment **34** had a modest effect on *QSOX1a* protein levels, reducing them by ~15% at a 20 μM concentration (~15% reduction) while having no effect on *QSOX1b* or *SQSTM1* protein levels.

As **34** had a very modest activity on *QSOX1a* protein levels, it was lead optimized by its conversion into a ribonuclease targeting chimera (RiboTAC; **36**, Figure 8B). RiboTACs comprise an RNA-binding module and a ribonuclease recruiter moiety. The RiboTAC binds inactive RNase L monomers endogenously present in cells, activates it by dimerizing the enzyme, and brings the activated RNase L dimer into close proximity of the RNA target such that it is cleaved. RiboTACs are catalytic, substoichiometric, and selective due to various factors including the inherent selectivity of the small molecule, RNase L’s substrate preferences, (113) and cellular localization of the target, among others. (108) Indeed, **34**’s binding site in *QSOX1a* is proximal to a preferred RNase L substrate (UNN). (113) RiboTAC **36** induced isoform-specific cleavage of *QSOX1a* mRNA and isoform-specific reduction of the *QSOX1a* protein in MDA-MB-231 cells. The compound also reduced cell proliferation, a phenotype associated with *QSOX1* expression.

These key studies lay a foundation for the discovery of fragments that bind cellular RNAs agnostically, providing a means to define the fragment interactome.

Selective 2′-Hydroxyl Acylation Analyzed by Primer Extension and Mutational Profiling (SHAPE-MaP)

SHAPE-MaP (selective 2′-hydroxyl acylation analyzed by primer extension and mutational profiling) is an RNA structure probing methodology that studies conformational changes in RNA structure upon compound binding at nucleotide resolution (Figure 9A). (114) SHAPE reagents react with ribose's 2′-hydroxyl group, reporting on the dynamics of the nucleotide. The site of modification is identified using a relaxed fidelity reverse transcriptase, which induces mutations at the site of the reaction. SHAPE profiles in the presence and absence of the small molecule are then compared. (115)

FBDD and SHAPE-MaP were first integrated to identify fragments that bind the TPP riboswitch. (2) Nucleotides with enhanced SHAPE reactivity (>20%) upon treatment with a fragment were further analyzed and assigned a *Z*-score. A fragment was determined to have a statistically significant altered SHAPE reactivity pattern if three or more nucleotides had *Z*-values greater than 2.7, which was determined by comparison of the Poisson counts. (116)

In brief, fragments were screened for binding an RNA construct comprising the aptamer domain of the TPP riboswitch and the 5′ UTR of Dengue virus, allowing identification of selective and nonselective binders. Of the 1,500 fragments screened by SHAPE-MaP, 41 fragments bound to either the TPP riboswitch or 5′ UTR of Dengue virus. A secondary validation of the hit compounds identified eight fragments, of which seven were selective for the riboswitch. The binding affinities of six hits were measured by ITC, where fragments demonstrated binding affinities in the range of 11 to 650 μM, and quinazoline (representative example **22**) emerged as a high-affinity binding scaffold (Figure 9B). Interestingly, fragment **22** also binds to the *E. coli ThiM* riboswitch (Figure 6).

With the goal of tethering two fragments together, a second round of screening with **22** bound to the TPP riboswitch alone was conducted to identify fragments that can bind to an adjacent site within the target. Of the 1500 fragments screened, five bound to the RNA in the presence of **22**. Interestingly, fragment **37** demonstrated cooperative binding with **22** (K_d = 3 mM), while a low-affinity interaction was observed (K_d > 10 mM) in the absence of **22**. Fragments **22** and **37** were then linked together to obtain **38**, which bound the TPP riboswitch with a K_d value of 620 nM (Figure 9B). Although the final compound, **38**, was able to inhibit conformational switching *in vitro* (K_{switch} = 68 μM, ~100-fold higher K_d), the binding affinity did not directly translate to functional activity.

In summary, this study demonstrated that SHAPE-MaP can identify fragments that bind the TPP riboswitch at adjacent sites and that linking them together increases the affinity. Importantly, this study demonstrated that SHAPE-Map can identify binding fragments and map their binding sites simultaneously in a high-throughput fashion. However, the reactivity bias of nucleotides and uncertainties associated with structural modeling can affect accurate mapping of the binding site.

Two-Dimensional Combinatorial Screening (2DCS)

As described before, one of the challenges in FBDD for RNAs is identification of conserved RNA regions that can be targeted using small molecules to modulate RNA function in a disease relevant system. This challenge is particularly evident, as most methods described above are target-specific with their utility usually validated with well-studied RNA targets. To expand the diversity of RNA molecules targetable with small molecular weight fragments, a target agnostic, selection-based, library-vs-library screening platform can be employed (Figure 10A). (117) Here, small molecules can be immobilized on an agarose coated plate covalently (117,118) or absorbed to the surface (termed AbsorbArray) (34) in a spatially defined manner. A radiolabeled RNA library containing thousands of RNA motifs, including internal loops, bulges, and hairpins, is then incubated with the microarray in the presence of excess competitor oligonucleotides to constrain interactions to the randomized region. RNAs bound to small molecules are then excised from the arrays and identified by RNA-seq analysis. The sequencing data are analyzed by high-throughput structure–activity relationships through sequencing (HiT-StARTS), a pipeline that calculates the statistical significance of the enrichment in selection studies, as compared to the starting library. (34) These privileged RNA motif–small molecule interactions define the molecular fingerprint for each fragment and are housed in a publicly available database named Inforna. (119) Any RNA of interest's secondary structure can be easily mined against this database to identify small molecules that bind the desired RNA structure.

Indeed, 2DCS selections and the Inforna platform have informed the design of various tethered RNA-binding modules to increase affinity and specificity. For example, querying the affinity landscapes for various small molecules against the structural elements comprising primary miR-96 (pri-miR-96) afforded two small molecules, **39** that binds the 5′C<u>G</u>A/3′U<u>G</u>G loop adjacent to the Drosha site and **40** that binds the miRNA's Drosha site (5′U<u>U</u>U/3′A<u>U</u>A) (120) (Figure 10B). (6) *In vitro* binding studies demonstrated that **40** binds 5′U<u>U</u>U/3′A<u>U</u>A with a K_d value of 1300 nM and **39** binds 5′C<u>G</u>A/3′U<u>G</u>G with a K_d value of 1500 nM. These two small molecule modules were linked to obtain dimer **41**, which binds pri-miR-96 with a K_d value of 85 nM (Figure 10B). Furthermore, linking the two modules increased the cellular potency, as assayed by inhibition of pri-miR-96 biogenesis in MDA-MB-231 TNBC cells (IC_{50} values of ~20 μM for **40** and ~50 nM for **41**). (6,120) Notably, the average molecular weight of compounds that have been housed in Inforna is 457 Da; thus, their dimerization affords molecules of relatively large molecular weights. These studies suggest, however, that a similar approach might be applied to fragments to afford potent molecules of low molecular weight.

As proof of principle that it is indeed possible to define the molecular fingerprints of fragments and apply this information to target RNA selectively, a 2,500-member, RNA-focused fragment library (250 Da average molecular weight) was studied for binding to 3 × 3 and 3 × 2 internal loop libraries (ILLs) via 2DCS. (22) Three fragments selectively bound RNA structures that comprise the two RNA libraries, the affinity landscapes of which were defined. Interestingly, fragment **42** was predicted to bind the Dicer site of the miR-372 precursor (pre-miR-372) with the highest affinity based on HiT-StARTS statistical analysis (Figure 10C). Indeed, **42** bound pre-miR-372 with a K_d value of 300 nM, a high-affinity

interaction for a fragment. Furthermore, **42** yielded bioactive interaction with pre-miR-372 in AGS, a gastric cancer cell line inhibiting the biogenesis of miR-372 with an IC_{50} value of ~1 μM. The fragment also de-repressed a downstream target of miR-372, large tumor suppressor kinase 2 (LATS2) at the mRNA and protein levels while also reducing cell proliferation and invasion phenotypes driven by aberrant expression of miR-372. (22)

This study demonstrated that drug-like low molecular weight compounds can in fact be studied using 2DCS and that the method can detect high-affinity binding interactions between fragments and RNA. Importantly, the fragment hit, **42**, was bioactive in cells without any optimization. Taken together, there is vast potential for studying large and diverse fragment libraries via 2DCS to identify new chemical scaffolds that bind RNAs.

In Silico Methods

Over the past two decades, various *in silico* strategies have been developed to support FBDD endeavors and subsequent fragment-to-lead optimization efforts. Among these approaches, docking has been widely used for hit identification due to its capability of screening large databases of fragments in a relatively short amount of time. The advantage of docking for hit identification is that both commercially available screening libraries with limited chemical space and virtual libraries can be screened, expanding the chemical diversity of identified hits. Although there are some concerns regarding the applicability of docking algorithms for fragment screening, it has been shown that there is no difference performance-wise between screening drug-like molecules and low molecular weight fragments (Figure 11A). (121−123) In the following example, the application of docking for fragment hit identification against a purine riboswitch (guanine riboswitch carrying a C74U mutation: GRA) is described (Figure 11B). (14) In this study, a high-resolution (1.7 Å) GRA crystal structure was used to screen a fragment library of 2,592 compounds. A series of compounds with the highest docking scores, reflecting those most likely to bind with the highest relative affinities, were selected for experimental evaluation. Four compounds were identified with binding affinities in the μM range, out of which two fragments represented novel scaffolds (**43**–**46**) (Figure 11B).

This study showed that a force-field-based docking, despite inaccuracies of the scoring functions, (124) can be applied successfully to screen different chemotypes against RNA targets. We are not aware of other examples of fragment-based virtual screening targeting RNAs, which suggests the need to expand and develop virtual screening strategies for fragment-based targeting of RNAs.

Conclusions

Targeting RNAs using small molecules is undoubtedly an important area of therapeutic interest, both for disease-causing or -associated RNAs and also for undruggable proteins by targeting the encoding mRNAs. Therefore, there is a crucial need to generate bioactive, drug-like small molecule ligands with favorable molecular properties for bioavailability. Thus, fragment-based approaches to identify small molecular weight, drug-like ligands for RNAs are important. As described in this review, much work is being done to develop new methodologies and to repurpose traditional methods toward fragment identification (Table 1). Other strategies that have demonstrated the potential to discover fragments include

surface plasmon resonance (SPR), (125) tethering, (126) and target-directed cycloaddition. (127) Future work includes expanding these methods to study new RNA targets, increasing the diversity of fragment libraires, and developing novel strategies for detecting low-affinity fragment interactions with RNAs.

The fragments themselves have favorable physicochemical properties (Table S1) affording drug-like properties (quantitative estimate of drug-likeness (QED) > 0.5). Although a few are bioactive (in some cases modestly), most fragments thus far have been incorporated into larger molecules, which reduces drug-likeness. As small molecule targeting of RNA is in its relative infancy compared to protein targets, parameters that describe drug-likeness and chemical space that is privileged for RNA binding have not yet been fully defined. Likewise, advances in protein-targeting, particularly PROTACs, suggest that drug-like space can indeed expand outside the traditional Rule of 5 guidelines. (128,129)

Although some of the fragments discussed herein have similarities with protein-targeting fragments, other studies have identified privileged scaffolds that are specific for RNA such as 2-phenylindole, 2-phenyl benzimidazole, 2-phenylimidazole, methylpyrimidine-2,4-diamine, etc. (130−132) RNA-binding compounds also have different physicochemical properties (Table S1) compared with the FDA-approved drugs including lower LogPs (octanol–water partition coefficient), (133) greater topological polar surface area, and more hydrogen bond donors. (5) These differences suggest that a more concentrated effort to discover RNA-targeting fragments could provide distinct scaffolds. Nevertheless, the fact that many familiar protein-targeting scaffolds and small molecules (23,134,135) also bind RNA provides an opportunity for drug repurposing, as we have shown that the receptor tyrosine kinase inhibitor Dovitinib can be reprogrammed to target an oncogenic miRNA. (134) Overall, this dual-binding presents a challenge and an opportunity and importantly points to the necessity of more rigorous analyses in drug discovery efforts to include RNA targets.

Supplementary Material

Refer to Web version on PubMed Central for supplementary material.

Acknowledgments

This work was funded by the U.S. National Institutes of Health (R35 NS116846, R01 CA249180, and P01 NS099114 to M.D.D.), the U.S. Department of Defense (W81XWH-19–1-0718 and W81XWH-20–1-0727), and the Muscular Dystrophy Association (Development Grant 963835 to A.T.).

Blessy M. Suresh

Blessy M. Suresh received her Master of Science in Chemistry from the National Institute of Science Education and Research, India, in 2017. After, she completed her doctoral studies in Chemical Biology in 2022 under the guidance of Prof. Matthew D. Disney at The Scripps Research Institute in Jupiter, Florida. Her thesis research focused on the identification of drug-like small molecules that bind RNAs and targeted degradation of RNAs. Currently, she is a Biophysics Scientist at Arrakis Therapeutics.

Amirhossein Taghavi studied physics in Luxembourg and received his Ph.D. in 2018 on modeling the extensionally driven transitions of DNA. In his postdoctoral research at Florida Atlantic University and (UF) Scripps Research, he has employed computational chemistry to design small molecules targeting RNA expanded repeats as well as combined theoretical and experimental approaches for hit identification for RNA targets.

Jessica L. Childs-Disney received her B.S. from Messiah College and her M.S. and Ph.D. from the University of Rochester. She completed postdoctoral studies at the Swiss Federal Institute of Technology (ETH), Zürich. Jessica was an Assistant Professor at Canisius College before taking on her current role as a Senior Staff Scientist at The Scripps Research Institute Florida and then The Herbert Wertheim UF Scripps Institute for Biomedical Innovation and Technology. Her expertise is in the field of RNA biochemistry, biophysics, and chemical biology.

Matthew D. Disney received his early schooling in the Baltimore Catholic School System, his B.S. from the University of Maryland, and his Ph.D. from the University of Rochester in Physical Chemistry under the guidance of Professor Douglas H. Turner. He completed postdoctoral training at the Massachusetts Institute of Technology and the Swiss Federal Institute of Technology (ETH; Zürich, Switzerland). Matt is a Professor in the Department of Chemistry at The Herbert Wertheim UF Scripps Institute for Biomedical Innovation and Technology (formerly Scripps Florida). His laboratory works in the area of small molecule targeting of RNA, addressing fundamental questions surrounding the molecular recognition of RNA folds by small molecules to study problems of biomedical importance.

Abbreviations Used

2DCS	2-dimensional combinatorial screening
ASO	antisense oligonucleotide
Chem-CLIP	chemical cross-linking and isolation by pull-down
Chem-CLIP-Frag-Map	chemical cross-linking and isolation by pull-down fragment mapping
CPMG	Carr–Purcell–Meiboom–Gill
DCC	dynamic combinatorial chemistry
DNA	deoxyribonucleic acid
ENCODE	Encyclopedia of DNA Elements
ESI	electrospray ionization
FAXS	fluorine chemical shift anisotropy and exchange for screening
FBDD	fragment-based drug discovery

FDA	US Food & Drug Administration
FFF	fully functionalized fragment
FT-ICR	Fourier transform ion cyclotron resonance
HCV	hepatitis C virus
HiT-StARTS	high-throughput structure–activity relationships through sequencing
HIV	human immunodeficiency virus
HTS	high-throughput screening
Kd	dissociation constant
ILL	internal loop library
IRES	internal ribosome entry site
ITC	isothermal titration calorimetry
lncRNA	long noncoding RNA
LogP	octanol–water partition coefficient
MD	molecular dynamics
MIC	minimum inhibitory concentration
miRNA	microRNA
MS	mass spectrometry
ncRNA	noncoding RNA
NMR	nuclear magnetic resonance
PSA	polar surface area
QED	quantitative estimate of drug-likeness
RB-DCC	resin-bound dynamic combinatorial chemistry
RNA	ribonucleic acid
SAM	S-adenosylmethionine
SAR	structure–activity relationship
SHAPE	selective 2′-hydroxyl acylation analyzed by primer extension
SHAPE-MaP	selective 2′-hydroxyl acylation analyzed by primer extension and mutational profiling

snRNA	small nuclear RNA
SPR	surface plasmon resonance
TAR	trans-activation response element
Tat	transactivator of transcription
UTR	untranslated region
WaterLOGSY	water-ligand observed via gradient spectroscopy

References

1. Zeiger M; Stark S; Kalden E; Ackermann B; Ferner J; Scheffer U; Shoja-Bazargani F; Erdel V; Schwalbe H; Gobel MW Fragment based search for small molecule inhibitors of HIV-1 Tat-TAR. Bioorg. Med. Chem. Lett. 2014, 24 (24), 5576–5580, DOI: 10.1016/j.bmcl.2014.11.004 [PubMed: 25466178]
2. Zeller MJ; Favorov O; Li K; Nuthanakanti A; Hussein D; Michaud A; Lafontaine DA; Busan S; Serganov A; Aube J. SHAPE-enabled fragment-based ligand discovery for RNA. Proc. Natl. Acad. Sci. U. S. A. 2022, 119 (20), e2122660119 DOI: 10.1073/pnas.2122660119
3. Lee MK; Bottini A; Kim M; Bardaro MF Jr.; Zhang Z; Pellecchia M; Choi BS; Varani G. A novel small-molecule binds to the influenza A virus RNA promoter and inhibits viral replication. Chem. Commun. 2014, 50 (3), 368–370, DOI: 10.1039/C3CC46973E
4. Binas O; de Jesus V; Landgraf T; Volklein AE; Martins J; Hymon D; Kaur Bains J; Berg H; Biedenbander T; Furtig B. 19F NMR-based fragment screening for 14 different biologically active RNAs and 10 DNA and protein counter-screens. Chembiochem 2021, 22 (2), 423–433, DOI: 10.1002/cbic.202000476 [PubMed: 32794266]
5. Suresh BM; Li W; Zhang P; Wang KW; Yildirim I; Parker CG; Disney MD A general fragment-based approach to identify and optimize bioactive ligands targeting RNA. Proc. Natl. Acad. Sci. U. S. A. 2020, 117 (52), 33197–33203, DOI: 10.1073/pnas.2012217117 [PubMed: 33318191]
6. Velagapudi SP; Cameron MD; Haga CL; Rosenberg LH; Lafitte M; Duckett DR; Phinney DG; Disney MD Design of a small molecule against an oncogenic noncoding RNA. Proc. Natl. Acad. Sci. U. S. A. 2016, 113 (21), 5898–5903, DOI: 10.1073/pnas.1523975113 [PubMed: 27170187]
7. Kirsch P; Hartman AM; Hirsch AKH; Empting M. Concepts and core principles of fragment-based drug design. Molecules 2019, 24 (23), 4309, DOI: 10.3390/molecules24234309 [PubMed: 31779114]
8. Cressina E; Chen L; Abell C; Leeper FJ; Smith AG Fragment screening against the thiamine pyrophosphate riboswitch thiM. Chem. Sci. 2011, 2 (1), 157–165, DOI: 10.1039/C0SC00406E
9. Clamp M; Fry B; Kamal M; Xie X; Cuff J; Lin MF; Kellis M; Lindblad-Toh K; Lander ES Distinguishing protein-coding and noncoding genes in the human genome. Proc. Natl. Acad. Sci. U. S. A. 2007, 104 (49), 19428–19433, DOI: 10.1073/pnas.0709013104 [PubMed: 18040051]
10. Wei JW; Huang K; Yang C; Kang CS Non-coding RNAs as regulators in epigenetics (Review). Oncol. Rep. 2017, 37 (1), 3–9, DOI: 10.3892/or.2016.5236 [PubMed: 27841002]
11. Mattick JS; Makunin IV Non-coding RNA. Hum. Mol. Genet. 2006, 15 (suppl_1), R17–R29, DOI: 10.1093/hmg/ddl046 [PubMed: 16651366]
12. Slack FJ; Chinnaiyan AM The Role of Non-coding RNAs in Oncology. Cell 2019, 179 (5), 1033–1055, DOI: 10.1016/j.cell.2019.10.017 [PubMed: 31730848]
13. Swayze EE; Jefferson EA; Sannes-Lowery KA; Blyn LB; Risen LM; Arakawa S; Osgood SA; Hofstadler SA; Griffey RH SAR by MS: a ligand based technique for drug lead discovery against structured RNA targets. J. Med. Chem. 2002, 45 (18), 3816–3819, DOI: 10.1021/jm0255466 [PubMed: 12190303]

14. Daldrop P; Reyes FE; Robinson DA; Hammond CM; Lilley DM; Batey RT; Brenk R. Novel ligands for a purine riboswitch discovered by RNA-ligand docking. Chem. Biol. 2011, 18 (3), 324–335, DOI: 10.1016/j.chembiol.2010.12.020 [PubMed: 21439477]
15. Disney MD; Angelbello AJ Rational design of small molecules targeting oncogenic noncoding RNAs from sequence. Acc. Chem. Res. 2016, 49 (12), 2698–2704, DOI: 10.1021/acs.accounts.6b00326 [PubMed: 27993012]
16. Rupaimoole R; Slack FJ MicroRNA therapeutics: towards a new era for the management of cancer and other diseases. Nat. Rev. Drug. Discovery 2017, 16 (3), 203–222, DOI: 10.1038/nrd.2016.246 [PubMed: 28209991]
17. Adams BD; Parsons C; Walker L; Zhang WC; Slack FJ Targeting noncoding RNAs in disease. J. Clin. Invest. 2017, 127 (3), 761–771, DOI: 10.1172/JCI84424 [PubMed: 28248199]
18. Hrdlickova B; de Almeida RC; Borek Z; Withoff S. Genetic variation in the non-coding genome: Involvement of micro-RNAs and long non-coding RNAs in disease. Biochim. Biophys. Acta 2014, 1842 (10), 1910–1922, DOI: 10.1016/j.bbadis.2014.03.011 [PubMed: 24667321]
19. McNaughton BR; Gareiss PC; Miller BL Identification of a selective small-molecule ligand for HIV-1 frameshift-inducing stem-loop RNA from an 11,325 member resin bound dynamic combinatorial library. J. Am. Chem. Soc. 2007, 129 (37), 11306–11307, DOI: 10.1021/ja072114h [PubMed: 17722919]
20. Bodoor K; Boyapati V; Gopu V; Boisdore M; Allam K; Miller J; Treleaven WD; Weldeghiorghis T; Aboul-ela F. Design and implementation of an ribonucleic acid (RNA) directed fragment library. J. Med. Chem. 2009, 52 (12), 3753–3761, DOI: 10.1021/jm9000659 [PubMed: 19445516]
21. Tam B; Sherf D; Cohen S; Eisdorfer SA; Perez M; Soffer A; Vilenchik D; Akabayov SR; Wagner G; Akabayov B. Discovery of small-molecule inhibitors targeting the ribosomal peptidyl transferase center (PTC) of M. tuberculosis. Chem. Sci. 2019, 10 (38), 8764–8767, DOI: 10.1039/C9SC02520K [PubMed: 31803448]
22. Suresh BM; Akahori Y; Taghavi A; Crynen G; Gibaut QMR; Li Y; Disney MD Low-molecular weight small molecules can potently bind RNA and affect oncogenic pathways in cells. J. Am. Chem. Soc. 2022, 144 (45), 20815–20824, DOI: 10.1021/jacs.2c08770 [PubMed: 36322830]
23. Tong Y; Gibaut QMR; Rouse W; Childs-Disney JL; Suresh BM; Abegg D; Choudhary S; Akahori Y; Adibekian A; Moss WN Transcriptome-wide mapping of small-molecule RNA-binding sites in cells informs an isoform-specific degrader of QSOX1 mRNA. J. Am. Chem. Soc. 2022, 144 (26), 11620–11625, DOI: 10.1021/jacs.2c01929 [PubMed: 35737519]
24. Borsi V; Calderone V; Fragai M; Luchinat C; Sarti N. Entropic contribution to the linking coefficient in fragment based drug design: a case study. J. Med. Chem. 2010, 53 (10), 4285–4289, DOI: 10.1021/jm901723z [PubMed: 20415416]
25. Crooke ST; Baker BF; Crooke RM; Liang XH Antisense technology: an overview and prospectus. Nat. Rev. Drug. Discovery 2021, 20 (6), 427–453, DOI: 10.1038/s41573-021-00162-z [PubMed: 33762737]
26. Kuijper EC; Bergsma AJ; Pijnappel W; Aartsma-Rus A. Opportunities and challenges for antisense oligonucleotide therapies. J. Inherit. Metab. Dis. 2021, 44 (1), 72–87, DOI: 10.1002/jimd.12251 [PubMed: 32391605]
27. Beck H; Harter M; Hass B; Schmeck C; Baerfacker L. Small molecules and their impact in drug discovery: A perspective on the occasion of the 125th anniversary of the Bayer Chemical Research Laboratory. Drug Discovery Today 2022, 27 (6), 1560–1574, DOI: 10.1016/j.drudis.2022.02.015 [PubMed: 35202802]
28. Vickers TA; Wyatt JR; Freier SM Effects of RNA secondary structure on cellular antisense activity. Nucleic Acids Res. 2000, 28 (6), 1340–1347, DOI: 10.1093/nar/28.6.1340 [PubMed: 10684928]
29. Hendrix DK; Brenner SE; Holbrook SR RNA structural motifs: building blocks of a modular biomolecule. Q. Rev. Biophys. 2005, 38 (3), 221–243, DOI: 10.1017/S0033583506004215 [PubMed: 16817983]
30. Moazed D; Noller HF Interaction of antibiotics with functional sites in 16S ribosomal RNA. Nature 1987, 327 (6121), 389–394, DOI: 10.1038/327389a0 [PubMed: 2953976]

31. Winkler W; Nahvi A; Breaker RR Thiamine derivatives bind messenger RNAs directly to regulate bacterial gene expression. Nature 2002, 419 (6910), 952–956, DOI: 10.1038/nature01145 [PubMed: 12410317]
32. Blount KF; Wang JX; Lim J; Sudarsan N; Breaker RR Antibacterial lysine analogs that target lysine riboswitches. Nat. Chem. Biol. 2007, 3 (1), 44–49, DOI: 10.1038/nchembio842 [PubMed: 17143270]
33. Angelbello AJ; Rzuczek SG; McKee KK; Chen JL; Olafson H; Cameron MD; Moss WN; Wang ET; Disney MD Precise small-molecule cleavage of an r(CUG) repeat expansion in a myotonic dystrophy mouse model. Proc. Natl. Acad. Sci. U. S. A. 2019, 116 (16), 7799–7804, DOI: 10.1073/pnas.1901484116 [PubMed: 30926669]
34. Velagapudi SP; Luo Y; Tran T; Haniff HS; Nakai Y; Fallahi M; Martinez GJ; Childs-Disney JL; Disney MD Defining RNA-small molecule affinity landscapes enables design of a small molecule inhibitor of an oncogenic noncoding RNA. ACS Cent. Sci. 2017, 3 (3), 205–216, DOI: 10.1021/acscentsci.7b00009 [PubMed: 28386598]
35. Zhang P; Park HJ; Zhang J; Junn E; Andrews RJ; Velagapudi SP; Abegg D; Vishnu K; Costales MG; Childs-Disney JL Translation of the intrinsically disordered protein alpha-synuclein is inhibited by a small molecule targeting its structured mRNA. Proc. Natl. Acad. Sci. U. S. A. 2020, 117 (3), 1457–1467, DOI: 10.1073/pnas.1905057117 [PubMed: 31900363]
36. Childs-Disney JL; Yang X; Gibaut QMR; Tong Y; Batey RT; Disney MD Targeting RNA structures with small molecules. Nat. Rev. Drug Discovery 2022, 21 (10), 736–762, DOI: 10.1038/s41573-022-00521-4 [PubMed: 35941229]
37. Congreve M; Carr R; Murray C; Jhoti HA 'rule of three' for fragment-based lead discovery?. Drug Discovery Today 2003, 8 (19), 876–877, DOI: 10.1016/S1359-6446(03)02831-9
38. Jencks WP On the attribution and additivity of binding energies. Proc. Natl. Acad. Sci. U. S. A. 1981, 78 (7), 4046–4050, DOI: 10.1073/pnas.78.7.4046 [PubMed: 16593049]
39. Krishnamurthy VM; Estroff LA; Whitesides GM Multivalency in Ligand Design. In Fragment-based Approaches in Drug Discovery; Methods and Principles in Medicinal Chemistry; WILEY-VCH Verlag GmbH & Co.: Weinheim, Germany, 2006; pp 11–53.
40. Mammen M; Choi SK; Whitesides GM Polyvalent Interactions in Biological Systems: Implications for Design and Use of Multivalent Ligands and Inhibitors. Angew. Chem., Int. Ed. Engl. 1998, 37 (20), 2754–2794, DOI: 10.1002/(SICI)1521-3773(19981102)37:20<2754::AID-ANIE2754>3.0.CO;2-3 [PubMed: 29711117]
41. Murray CW; Verdonk ML The consequences of translational and rotational entropy lost by small molecules on binding to proteins. J. Comput. Aided Mol. Des. 2002, 16 (10), 741–753, DOI: 10.1023/A:1022446720849 [PubMed: 12650591]
42. Ferenczy GG; Keseru GM Thermodynamic profiling for fragment-based lead discovery and optimization. Expert Opin. Drug Discovery 2020, 15 (1), 117–129, DOI: 10.1080/17460441.2020.1691166
43. Shuker SB; Hajduk PJ; Meadows RP; Fesik SW Discovering high-affinity ligands for proteins: SAR by NMR. Science 1996, 274 (5292), 1531–1534, DOI: 10.1126/science.274.5292.1531 [PubMed: 8929414]
44. Lamoree B; Hubbard RE Current perspectives in fragment-based lead discovery (FBLD). Essays Biochem. 2017, 61 (5), 453–464, DOI: 10.1042/EBC20170028 [PubMed: 29118093]
45. Scott DE; Coyne AG; Hudson SA; Abell C. Fragment-based approaches in drug discovery and chemical biology. Biochemistry 2012, 51 (25), 4990–5003, DOI: 10.1021/bi3005126 [PubMed: 22697260]
46. Souers AJ; Leverson JD; Boghaert ER; Ackler SL; Catron ND; Chen J; Dayton BD; Ding H; Enschede SH; Fairbrother WJ ABT-199, a potent and selective BCL-2 inhibitor, achieves antitumor activity while sparing platelets. Nat. Med. 2013, 19 (2), 202–208, DOI: 10.1038/nm.3048 [PubMed: 23291630]
47. Bollag G; Tsai J; Zhang J; Zhang C; Ibrahim P; Nolop K; Hirth P. Vemurafenib: the first drug approved for BRAF-mutant cancer. Nat. Rev. Drug. Discovery 2012, 11 (11), 873–886, DOI: 10.1038/nrd3847 [PubMed: 23060265]

48. Schoepfer J; Jahnke W; Berellini G; Buonamici S; Cotesta S; Cowan-Jacob SW; Dodd S; Drueckes P; Fabbro D; Gabriel T. Discovery of Asciminib (ABL001), an allosteric inhibitor of the tyrosine kinase activity of BCR-ABL1. J. Med. Chem. 2018, 61 (18), 8120–8135, DOI: 10.1021/acs.jmedchem.8b01040 [PubMed: 30137981]
49. Perera TPS; Jovcheva E; Mevellec L; Vialard J; De Lange D; Verhulst T; Paulussen C; Van De Ven K; King P; Freyne E. Discovery and pharmacological characterization of JNJ-42756493 (Erdafitinib), a functionally selective small-molecule FGFR family inhibitor. Mol. Cancer Ther. 2017, 16 (6), 1010–1020, DOI: 10.1158/1535-7163.MCT-16-0589 [PubMed: 28341788]
50. Lamb YN Pexidartinib: first approval. Drugs 2020, 80 (4), 447, DOI: 10.1007/s40265-020-01280-5 [PubMed: 32112350]
51. Lanman BA; Allen JR; Allen JG; Amegadzie AK; Ashton KS; Booker SK; Chen JJ; Chen N; Frohn MJ; Goodman G. Discovery of a covalent inhibitor of KRAS(G12C) (AMG 510) for the treatment of solid tumors. J. Med. Chem. 2020, 63 (1), 52–65, DOI: 10.1021/acs.jmedchem.9b01180 [PubMed: 31820981]
52. Fairbrother WJ; Leverson JD; Sampath D; Souers AJ Discovery and Development of Venetoclax, a Selective Antagonist of BCL-2. Successful Drug Discovery; eds Fischer J; Klein C; Childers WE, Eds.; Wiley−VCH: Hoboken, N.J., 2019, pp 225–245, DOI: 10.1002/9783527814695.ch9.
53. Erlanson DA; Fesik SW; Hubbard RE; Jahnke W; Jhoti H. Twenty years on: the impact of fragments on drug discovery. Nat. Rev. Drug. Discovery 2016, 15 (9), 605–619, DOI: 10.1038/nrd.2016.109 [PubMed: 27417849]
54. Guan L; Disney MD Recent advances in developing small molecules targeting RNA. ACS Chem. Biol. 2012, 7 (1), 73–86, DOI: 10.1021/cb200447r
55. Matsui M; Corey DR Non-coding RNAs as drug targets. Nat. Rev. Drug Discovery 2017, 16 (3), 167–179, DOI: 10.1038/nrd.2016.117 [PubMed: 27444227]
56. Davis BJ; Roughley SD Fragment-Based Lead Discovery. Platform Technologies in Drug Discovery and Validation; Annual Reports in Medicinal Chemistry; 2017; pp 371–439.
57. Erlanson DA; Davis BJ; Jahnke W. Fragment-based drug discovery: advancing fragments in the absence of crystal structures. Cell Chem. Biol. 2019, 26 (1), 9–15, DOI: 10.1016/j.chembiol.2018.10.001 [PubMed: 30482678]
58. Pahl A; Waldmann H; Kumar K. Exploring natural product fragments for drug and probe discovery. Chimia 2017, 71 (10), 653–660, DOI: 10.2533/chimia.2017.653 [PubMed: 29070410]
59. Nasiri HR; Bell NM; McLuckie KI; Husby J; Abell C; Neidle S; Balasubramanian S. Targeting a c-MYC G-quadruplex DNA with a fragment library. Chem. Commun. 2014, 50 (14), 1704–1707, DOI: 10.1039/C3CC48390H
60. Mortenson PN; Erlanson DA; de Esch IJP; Jahnke W; Johnson CN Fragment-to-Lead Medicinal Chemistry Publications in 2017. J. Med. Chem. 2019, 62 (8), 3857–3872, DOI: 10.1021/acs.jmedchem.8b01472 [PubMed: 30462504]
61. Lundquist KP; Panchal V; Gotfredsen CH; Brenk R; Clausen MH Fragment-based drug discovery for RNA targets. ChemMedChem. 2021, 16 (17), 2588–2603, DOI: 10.1002/cmdc.202100324 [PubMed: 34101375]
62. Seth PP; Miyaji A; Jefferson EA; Sannes-Lowery KA; Osgood SA; Propp SS; Ranken R; Massire C; Sampath R; Ecker DJ SAR by MS: discovery of a new class of RNA-binding small molecules for the hepatitis C virus: internal ribosome entry site IIA subdomain. J. Med. Chem. 2005, 48 (23), 7099–7102, DOI: 10.1021/jm050815o [PubMed: 16279767]
63. Li Q. Application of fragment-based drug discovery to versatile targets. Front. Mol. Biosci. 2020, 7, 180, DOI: 10.3389/fmolb.2020.00180 [PubMed: 32850968]
64. Shortridge MD; Varani G. Efficient NMR screening approach to discover small molecule fragments binding structured RNA. ACS Med. Chem. Lett. 2021, 12 (8), 1253–1260, DOI: 10.1021/acsmedchemlett.1c00109
65. Sreeramulu S; Richter C; Berg H; Wirtz Martin MA; Ceylan B; Matzel T; Adam J; Altincekic N; Azzaoui K; Bains JK Exploring the druggability of conserved RNA regulatory elements in the SARS-CoV-2 genome. Angew. Chem., Int. Ed. Engl. 2021, 60 (35), 19191–19200, DOI: 10.1002/anie.202103693 [PubMed: 34161644]

66. Mercier KA; Shortridge MD; Powers R. A multi-step NMR screen for the identification and evaluation of chemical leads for drug discovery. Comb. Chem. High Throughput Screen. 2009, 12 (3), 285–295, DOI: 10.2174/138620709787581738 [PubMed: 19275534]

67. Ortega-Roldan JL; Jensen MR; Brutscher B; Azuaga AI; Blackledge M; van Nuland NA Accurate characterization of weak macromolecular interactions by titration of NMR residual dipolar couplings: application to the CD2AP SH3-C:ubiquitin complex. Nucleic Acids Res. 2009, 37 (9), e70, DOI: 10.1093/nar/gkp211 [PubMed: 19359362]

68. Dalvit C. NMR methods in fragment screening: theory and a comparison with other biophysical techniques. Drug Discovery Today 2009, 14 (21–22), 1051–1057, DOI: 10.1016/j.drudis.2009.07.013 [PubMed: 19716431]

69. Liu J; Gao J; Li F; Ma R; Wei Q; Wang A; Wu J; Ruan K. NMR characterization of weak interactions between RhoGDI2 and fragment screening hits. Biochim. Biophys. Acta Gen. Subj. 2017, 1861 (1 Pt A), 3061–3070, DOI: 10.1016/j.bbagen.2016.10.003 [PubMed: 27721047]

70. Hajduk PJ; Olejniczak ET; Fesik SW One-dimensional relaxation- and diffusion-edited NMR methods for screening compounds that bind to macromolecules. J. Am. Chem. Soc. 1997, 119 (50), 12257–12261, DOI: 10.1021/ja9715962

71. Jahnke W. Spin labels as a tool to identify and characterize protein-ligand interactions by NMR spectroscopy. Chembiochem 2002, 3 (2–3), 167–173, DOI: 10.1002/1439-7633(20020301)3:2/3<167::AID-CBIC167>3.0.CO;2-S [PubMed: 11921394]

72. Ma R; Wang P; Wu J; Ruan K. Process of fragment-based lead discovery-a perspective from NMR. Molecules 2016, 21 (7), 854, DOI: 10.3390/molecules21070854 [PubMed: 27438813]

73. Davidson A; Begley DW; Lau C; Varani G. A small-molecule probe induces a conformation in HIV TAR RNA capable of binding drug-like fragments. J. Mol. Biol. 2011, 410 (5), 984–996, DOI: 10.1016/j.jmb.2011.03.039 [PubMed: 21763501]

74. Dalvit C; Pevarello P; Tato M; Veronesi M; Vulpetti A; Sundstrom M. Identification of compounds with binding affinity to proteins via magnetization transfer from bulk water. J. Biomol. NMR 2000, 18 (1), 65–68, DOI: 10.1023/A:1008354229396 [PubMed: 11061229]

75. Dalvit C; Fagerness PE; Hadden DT; Sarver RW; Stockman BJ Fluorine-NMR experiments for high-throughput screening: theoretical aspects, practical considerations, and range of applicability. J. Am. Chem. Soc. 2003, 125 (25), 7696–7703, DOI: 10.1021/ja034646d [PubMed: 12812511]

76. Lombès T; Moumné R; Larue V; Prost E; Catala M; Lecourt T; Dardel F; Micouin L; Tisné C. Investigation of RNA–ligand interactions by 19F NMR spectroscopy using fluorinated probes. Angew. Chem., Int. Ed. 2012, 51 (38), 9530–9534, DOI: 10.1002/anie.201204083

77. Moumné R; Catala M; Larue V; Micouin L; Tisné C. Fragment-based design of small RNA binders: promising developments and contribution of NMR. Biochimie 2012, 94 (7), 1607–1619, DOI: 10.1016/j.biochi.2012.02.002 [PubMed: 22353243]

78. Schwieters CD; Bermejo GA; Clore GM Xplor-NIH for molecular structure determination from NMR and other data sources. Protein Sci. 2018, 27 (1), 26–40, DOI: 10.1002/pro.3248 [PubMed: 28766807]

79. Schwieters CD; Kuszewski JJ; Tjandra N; Clore GM The Xplor-NIH NMR molecular structure determination package. J. Magn. Reson. 2003, 160 (1), 65–73, DOI: 10.1016/S1090-7807(02)00014-9 [PubMed: 12565051]

80. Schwieters CD; Kuszewski JJ; Clore GM Using Xplor-NIH for NMR molecular structure determination. Prog. Nucl. Magn. Reson. Spectrosc. 2006, 48 (1), 47–62, DOI: 10.1016/j.pnmrs.2005.10.001

81. Larsen FH; Jakobsen HJ; Ellis PD; Nielsen NC Sensitivity-enhanced quadrupolar-echo NMR of half-integer quadrupolar nuclei. Magnitudes and relative orientation of chemical shielding and quadrupolar coupling tensors. J. Phys. Chem. A 1997, 101 (46), 8597–8606, DOI: 10.1021/jp971547b

82. Schnieders R; Keyhani S; Schwalbe H; Furtig B. More than proton detection-new Avenues for NMR Spectroscopy of RNA. Chemistry 2020, 26 (1), 102–113, DOI: 10.1002/chem.201903355 [PubMed: 31454110]

83. Pervushin K; Riek R; Wider G; Wuthrich K. Attenuated T2 relaxation by mutual cancellation of dipole-dipole coupling and chemical shift anisotropy indicates an avenue to NMR structures of

very large biological macromolecules in solution. Proc. Natl. Acad. Sci. U. S. A. 1997, 94 (23), 12366–12371, F DOI: 10.1073/pnas.94.23.12366 [PubMed: 9356455]

84. Dalvit C; Fogliatto G; Stewart A; Veronesi M; Stockman B. WaterLOGSY as a method for primary NMR screening: practical aspects and range of applicability. J. Biomol. NMR 2001, 21 (4), 349–359, DOI: 10.1023/A:1013302231549 [PubMed: 11824754]
85. Hofstadler SA; Sannes-Lowery KA Applications of ESI-MS in drug discovery: interrogation of noncovalent complexes. Nat. Rev. Drug. Discovery 2006, 5 (7), 585–595, DOI: 10.1038/nrd2083 [PubMed: 16816839]
86. Hofstadler SA; Griffey RH Analysis of noncovalent complexes of DNA and RNA by mass spectrometry. Chem. Rev. 2001, 101 (2), 377–390, DOI: 10.1021/cr990105o [PubMed: 11712252]
87. Griffey RH; Sannes-Lowery KA; Drader JJ; Mohan V; Swayze EE; Hofstadler SA Characterization of low-affinity complexes between RNA and small molecules using electrospray ionization mass spectrometry. J. Am. Chem. Soc. 2000, 122 (41), 9933–9938, DOI: 10.1021/ja0017108
88. Hofstadler SA; Sannes-Lowery KA; Crooke ST; Ecker DJ; Sasmor H; Manalili S; Griffey RH Multiplexed screening of neutral mass-tagged RNA targets against ligand libraries with electrospray ionization FT-ICR MS: a paradigm for high-throughput affinity screening. Anal. Chem. 1999, 71 (16), 3436–3440, DOI: 10.1021/ac990262n [PubMed: 10464476]
89. Griffey RH; Hofstadler SA; Sannes-Lowery KA; Ecker DJ; Crooke ST Determinants of aminoglycoside-binding specificity for rRNA by using mass spectrometry. Proc. Natl. Acad. Sci. U. S. A. 1999, 96 (18), 10129–10133, DOI: 10.1073/pnas.96.18.10129 [PubMed: 10468574]
90. Conn GL; Draper DE; Lattman EE; Gittis AG Crystal structure of a conserved ribosomal protein-RNA complex. Science 1999, 284 (5417), 1171–1174, DOI: 10.1126/science.284.5417.1171 [PubMed: 10325228]
91. Jefferson EA; Seth PP; Robinson DE; Winter DK; Miyaji A; Risen LM; Osgood SA; Bertrand M; Swayze EE Optimizing the antibacterial activity of a lead structure discovered by ″SAR by MS″ technology. Bioorg. Med. Chem. Lett. 2004, 14 (21), 5257–5261, DOI: 10.1016/j.bmcl.2004.08.033 [PubMed: 15454207]
92. McNaughton BR; Miller BL Resin-bound dynamic combinatorial chemistry. Org. Lett. 2006, 8 (9), 1803–1806, DOI: 10.1021/ol060330+ [PubMed: 16623555]
93. McAnany JD; Miller BL Chapter Four - Dynamic combinatorial chemistry as a rapid method for discovering sequence-selective RNA-binding compounds. Methods Enzymol. 2019, 623, 67–84, DOI: 10.1016/bs.mie.2019.05.012 [PubMed: 31239058]
94. Frei P; Hevey R; Ernst B. Dynamic combinatorial chemistry: a new methodology comes of age. Chemistry 2019, 25 (1), 60–73, DOI: 10.1002/chem.201803365 [PubMed: 30204930]
95. Hilimire TA; Chamberlain JM; Anokhina V; Bennett RP; Swart O; Myers JR; Ashton JM; Stewart RA; Featherston AL; Gates K. HIV-1 frameshift RNA-targeted triazoles inhibit propagation of replication-competent and multi-drug-resistant HIV in muman cells. ACS Chem. Biol. 2017, 12 (6), 1674–1682, DOI: 10.1021/acschembio.7b00052
96. Anokhina VS; Miller BL Targeting ribosomal frameshifting as an antiviral strategy: from HIV-1 to SARS-CoV-2. Acc. Chem. Res. 2021, 54 (17), 3349–3361, DOI: 10.1021/acs.accounts.1c00316 [PubMed: 34403258]
97. Gareiss PC; Sobczak K; McNaughton BR; Palde PB; Thornton CA; Miller BL Dynamic combinatorial selection of molecules capable of inhibiting the (CUG) repeat RNA-MBNL1 interaction in vitro: discovery of lead compounds targeting myotonic dystrophy (DM1). J. Am. Chem. Soc. 2008, 130 (48), 16254–16261, DOI: 10.1021/ja804398y [PubMed: 18998634]
98. Lopez-Senin P; Gomez-Pinto I; Grandas A; Marchan V. Identification of ligands for the Tau exon 10 splicing regulatory element RNA by using dynamic combinatorial chemistry. Chemistry 2011, 17 (6), 1946–1953, DOI: 10.1002/chem.201002065 [PubMed: 21274946]
99. Chaires JB Structural Selectivity of Drug-Nucleic Acid Interactions Probed by Competition Dialysis. In DNA Binders and Related Subjects; Waring MJ, Chaires JB, Eds.; Springer: Berlin, Heidelberg, 2005; pp 33–53.

100. Chen L; Cressina E; Leeper FJ; Smith AG; Abell C. A fragment-based approach to identifying ligands for riboswitches. ACS Chem. Biol. 2010, 5 (4), 355–358, DOI: 10.1021/cb9003139 [PubMed: 20158266]
101. Breaker RR Riboswitches and translation Control. Cold Spring Harb. Perspect. Biol. 2018, 10 (11), a032797 DOI: 10.1101/cshperspect.a032797
102. Warner KD; Homan P; Weeks KM; Smith AG; Abell C; Ferre-D'Amare AR Validating fragment-based drug discovery for biological RNAs: lead fragments bind and remodel the TPP riboswitch specifically. Chem. Biol. 2014, 21 (5), 591–595, DOI: 10.1016/j.chembiol.2014.03.007 [PubMed: 24768306]
103. Weeks KM; Ampe C; Schultz SC; Steitz TA; Crothers DM Fragments of the HIV-1 Tat protein specifically bind TAR RNA. Science 1990, 249 (4974), 1281–1285, DOI: 10.1126/science.2205002 [PubMed: 2205002]
104. Matsumoto C; Hamasaki K; Mihara H; Ueno A. A high-throughput screening utilizing intramolecular fluorescence resonance energy transfer for the discovery of the molecules that bind HIV-1 TAR RNA specifically. Bioorg. Med. Chem. Lett. 2000, 10 (16), 1857–1861, DOI: 10.1016/S0960-894X(00)00359-0 [PubMed: 10969985]
105. Parker CG; Galmozzi A; Wang Y; Correia BE; Sasaki K; Joslyn CM; Kim AS; Cavallaro CL; Lawrence RM; Johnson SR Ligand and target discovery by fragment-based screening in human cells. Cell 2017, 168 (3), 527–541, DOI: 10.1016/j.cell.2016.12.029 [PubMed: 28111073]
106. Selcuklu SD; Donoghue MT; Spillane C. miR-21 as a key regulator of oncogenic processes. Biochem. Soc. Trans. 2009, 37 (4), 918–925, DOI: 10.1042/BST0370918 [PubMed: 19614619]
107. Krichevsky AM; Gabriely G. miR-21: a small multi-faceted RNA.. J. Cell. Mol. Med. 2009, 13 (1), 39–53, DOI: 10.1111/j.1582-4934.2008.00556.x [PubMed: 19175699]
108. Costales MG; Aikawa H; Li Y; Childs-Disney JL; Abegg D; Hoch DG; Velagapudi S; Nakai Y; Khan T; Wang KW Small-molecule targeted recruitment of a nuclease to cleave an oncogenic RNA in a mouse model of metastatic cancer. Proc. Natl. Acad. Sci. U. S. A. 2020, 117 (5), 2406–2411, DOI: 10.1073/pnas.1914286117 [PubMed: 31964809]
109. https://github.com/jsh58/Genrich (acesssed Jan 9, 2022).
110. Andrews RJ; Roche J; Moss WN ScanFold: an approach for genome-wide discovery of local RNA structural elements-applications to Zika virus and HIV. PeerJ. 2018, 6, e6136 DOI: 10.7717/peerj.6136 [PubMed: 30627482]
111. Katchman BA; Ocal IT; Cunliffe HE; Chang YH; Hostetter G; Watanabe A; LoBello J; Lake DF Expression of quiescin sulfhydryl oxidase 1 is associated with a highly invasive phenotype and correlates with a poor prognosis in Luminal B breast cancer. Breast Cancer Res. 2013, 15 (2), R28, DOI: 10.1186/bcr3407 [PubMed: 23536962]
112. Sung HJ; Ahn JM; Yoon YH; Na SS; Choi YJ; Kim YI; Lee SY; Lee EB; Cho S; Cho JY Quiescin Sulfhydryl Oxidase 1 (QSOX1) secreted by lung cancer cells promotes cancer metastasis. Int. J. Mol. Sci. 2018, 19 (10), 3213, DOI: 10.3390/ijms19103213 [PubMed: 30336636]
113. Han Y; Donovan J; Rath S; Whitney G; Chitrakar A; Korennykh A. Structure of human RNase L reveals the basis for regulated RNA decay in the IFN response. Science 2014, 343 (6176), 1244–1248, DOI: 10.1126/science.1249845 [PubMed: 24578532]
114. Siegfried NA; Busan S; Rice GM; Nelson JA; Weeks KM RNA motif discovery by SHAPE and mutational profiling (SHAPE-MaP). Nat. Methods 2014, 11 (9), 959–965, DOI: 10.1038/nmeth.3029 [PubMed: 25028896]
115. Chamberlin SI; Weeks KM Mapping local nucleotide flexibility by selective acylation of 2 '-amine substituted RNA. J. Am. Chem. Soc. 2000, 122 (2), 216–224, DOI: 10.1021/ja9914137
116. Woolson RF; Clarke WR Statistical Methods for the Analysis of Biomedical Data; John Wiley & Sons: 2011.
117. Disney MD; Labuda LP; Paul DJ; Poplawski SG; Pushechnikov A; Tran T; Velagapudi SP; Wu M; Childs-Disney JL Two-dimensional combinatorial screening identifies specific aminoglycoside-RNA internal loop partners. J. Am. Chem. Soc. 2008, 130 (33), 11185–11194, DOI: 10.1021/ja803234t [PubMed: 18652457]

118. Tran T; Disney MD Two-dimensional combinatorial screening of a bacterial rRNA A-site-like motif library: defining privileged asymmetric internal loops that bind aminoglycosides. Biochemistry 2010, 49 (9), 1833–1842, DOI: 10.1021/bi901998m [PubMed: 20108982]

119. Disney MD; Winkelsas AM; Velagapudi SP; Southern M; Fallahi M; Childs-Disney JL Inforna 2.0: a platform for the sequence-based design of small molecules targeting structured RNAs. ACS Chem. Biol. 2016, 11 (6), 1720–1728, DOI: 10.1021/acschembio.6b00001 [PubMed: 27097021]

120. Velagapudi SP; Gallo SM; Disney MD Sequence-based design of bioactive small molecules that target precursor microRNAs. Nat. Chem. Biol. 2014, 10 (4), 291–297, DOI: 10.1038/nchembio.1452 [PubMed: 24509821]

121. Verdonk ML; Hartshorn MJ Structure-guided fragment screening for lead discovery. Curr. Opin. Drug Discovery Dev. 2004, 7 (4), 404–410

122. Joseph-McCarthy D; Campbell AJ; Kern G; Moustakas D. Fragment-based lead discovery and design. J. Chem. Inf. Model. 2014, 54 (3), 693–704, DOI: 10.1021/ci400731w [PubMed: 24490951]

123. Kumar A; Voet A; Zhang KY Fragment based drug design: from experimental to computational approaches. Curr. Med. Chem. 2012, 19 (30), 5128–5147, DOI: 10.2174/092986712803530467 [PubMed: 22934764]

124. Wu G; Robertson DH; Brooks CL 3rd; Vieth M. Detailed analysis of grid-based molecular docking: A case study of CDOCKER-A CHARMm-based MD docking algorithm. J. Comput. Chem. 2003, 24 (13), 1549–1562, DOI: 10.1002/jcc.10306 [PubMed: 12925999]

125. Arney JW; Weeks KM RNA-ligand interactions quantified by surface plasmon resonance with reference subtraction. Biochemistry 2022, 61 (15), 1625–1632, DOI: 10.1021/acs.biochem.2c00177 [PubMed: 35802500]

126. Tran K; Arkin MR; Beal PA Tethering in RNA: an RNA-binding fragment discovery tool. Molecules 2015, 20 (3), 4148–4161, DOI: 10.3390/molecules20034148 [PubMed: 25749683]

127. Paul R; Dutta D; Paul R; Dash J. Target-directed azide-alkyne cycloaddition for assembling HIV-1 TAR RNA binding ligands. Angew. Chem., Int. Ed. Engl. 2020, 59 (30), 12407–12411, DOI: 10.1002/anie.202003461 [PubMed: 32329147]

128. Lipinski CA; Lombardo F; Dominy BW; Feeney PJ Experimental and computational approaches to estimate solubility and permeability in drug discovery and development settings. Adv. Drug Delivery Rev. 2001, 46 (1–3), 3–26, DOI: 10.1016/S0169-409X(00)00129-0

129. DeGoey DA; Chen H-J; Cox PB; Wendt MD Beyond the Rule of 5: Lessons Learned from AbbVie's Drugs and Compound Collection. J. Med. Chem. 2018, 61 (7), 2636–2651, DOI: 10.1021/acs.jmedchem.7b00717 [PubMed: 28926247]

130. Parsons J; Castaldi MP; Dutta S; Dibrov SM; Wyles DL; Hermann T. Conformational inhibition of the hepatitis C virus internal ribosome entry site RNA. Nat. Chem. Biol. 2009, 5 (11), 823–825, DOI: 10.1038/nchembio.217 [PubMed: 19767736]

131. Murchie AI; Davis B; Isel C; Afshar M; Drysdale MJ; Bower J; Potter AJ; Starkey ID; Swarbrick TM; Mirza S. Structure-based drug design targeting an inactive RNA conformation: exploiting the flexibility of HIV-1 TAR RNA. J. Mol. Biol. 2004, 336 (3), 625–638, DOI: 10.1016/j.jmb.2003.12.028 [PubMed: 15095977]

132. Foloppe N; Chen IJ; Davis B; Hold A; Morley D; Howes R. A structure-based strategy to identify new molecular scaffolds targeting the bacterial ribosomal A-site. Bioorg. Med. Chem. 2004, 12 (5), 935–947, DOI: 10.1016/j.bmc.2003.12.023 [PubMed: 14980606]

133. Morgan BS; Forte JE; Culver RN; Zhang Y; Hargrove AE Discovery of key physicochemical, structural, and spatial properties of RNA-targeted bioactive ligands. Angew. Chem., Int. Ed. Engl. 2017, 56 (43), 13498–13502, DOI: 10.1002/anie.201707641 [PubMed: 28810078]

134. Zhang P; Liu X; Abegg D; Tanaka T; Tong Y; Benhamou RI; Baisden J; Crynen G; Meyer SM; Cameron MD Reprogramming of protein-targeted small-molecule medicines to RNA by ribonuclease recruitment. J. Am. Chem. Soc. 2021, 143 (33), 13044–13055, DOI: 10.1021/jacs.1c02248 [PubMed: 34387474]

135. Velagapudi SP; Costales MG; Vummidi BR; Nakai Y; Angelbello AJ; Tran T; Haniff HS; Matsumoto Y; Wang ZF; Chatterjee AK Approved anti-cancer drugs target oncogenic non-

coding RNAs. Cell Chem. Biol. 2018, 25 (9), 1086–1094, DOI: 10.1016/j.chembiol.2018.05.015 [PubMed: 30251629]

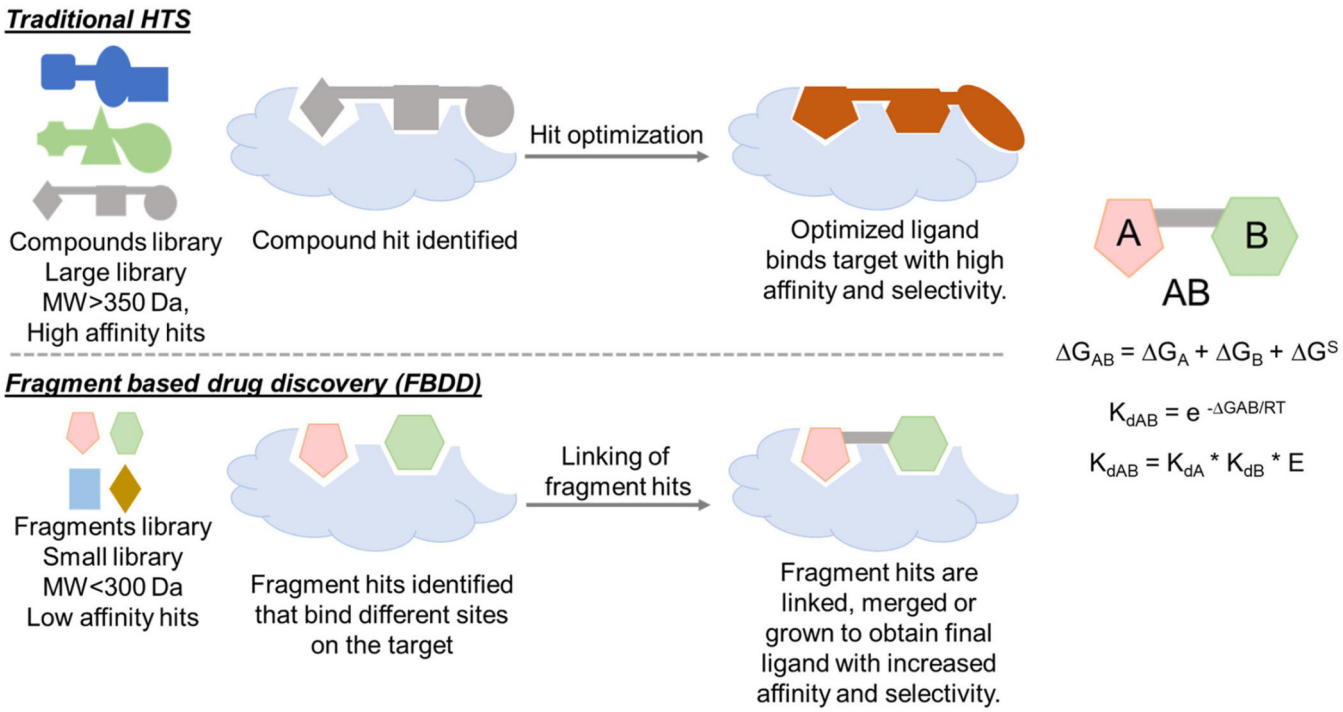

Figure 1. An overview of fragment-based drug discovery (FBDD).

Schematic for traditional high-throughput screening (HTS) vs FBDD (left). In traditional HTS, large compound libraries are screened against a target of interest to obtain hits that are then optimized to yield high affinity, selective ligands. In fragment-based drug discovery (FBDD), small molecular weight fragments are screened against a target library to obtain hits that bind different sites on the target. (7) Two fragments that bind an adjacent site on a target are then linked, merged, or grown to obtain a final ligand with increased affinity and selectivity. Thermodynamic parameters defining the linking fragments: ΔG_{AB}, free energy of binding of assembled ligand; ΔG_A, free energy of binding of fragment A; ΔG_B, free energy of binding of fragment B; ΔG^S, connection Gibbs energy; K_{dAB}, dissociation constant of assembled ligand; K_{dA}, dissociation constant of fragment A; K_{dB}, dissociation constant of fragment B; E, linking coefficient (right). (24)

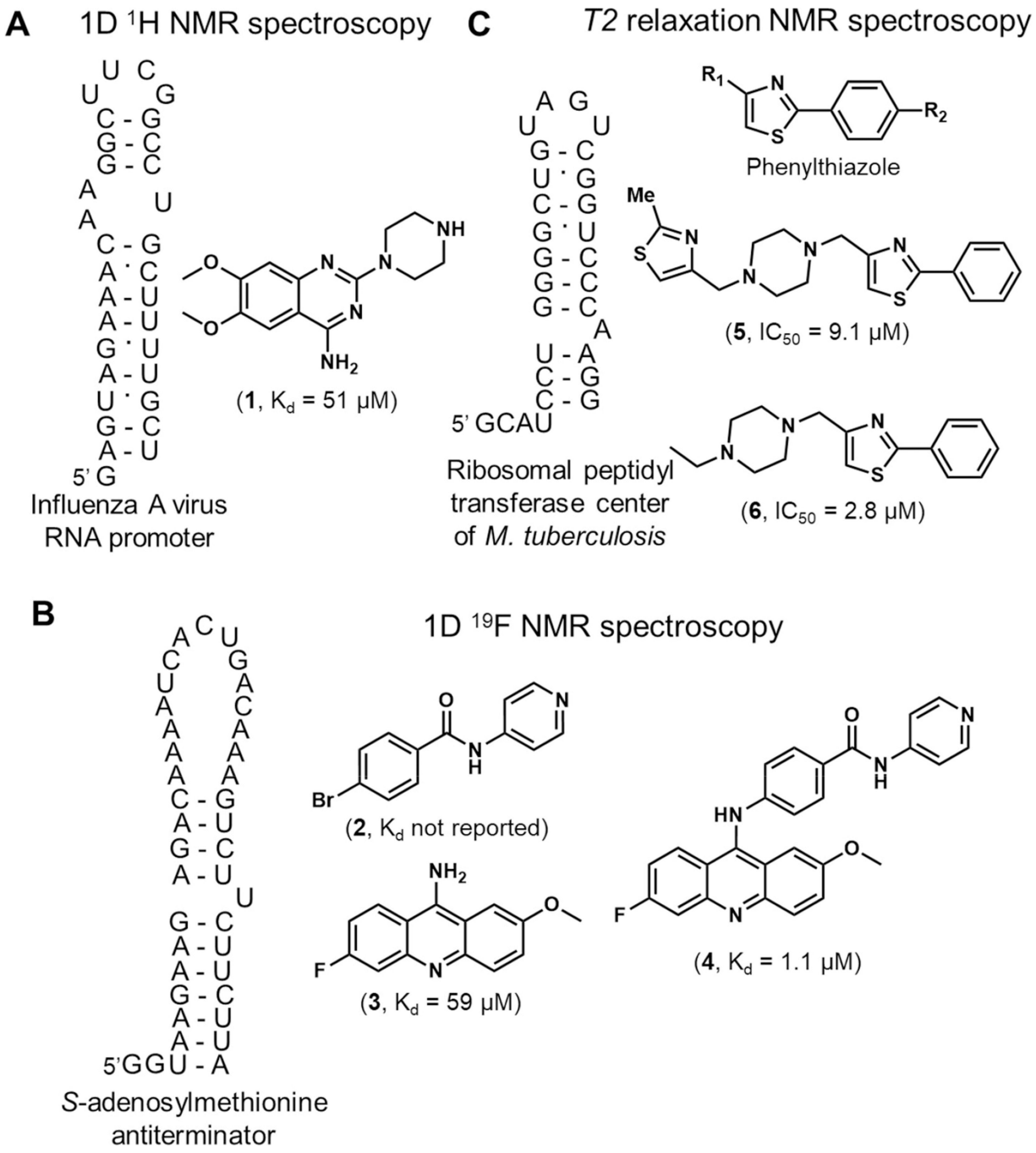

Figure 2. NMR spectroscopy methods to identify fragments that bind RNAs.

Secondary structures of RNA targets and chemical structures of fragment hits and optimized compounds by (A) 1D ^{1}H NMR spectroscopy, (3) (B) 1D ^{19}F NMR spectroscopy, (4) and (C) T_2 relaxation NMR spectroscopy. (21)

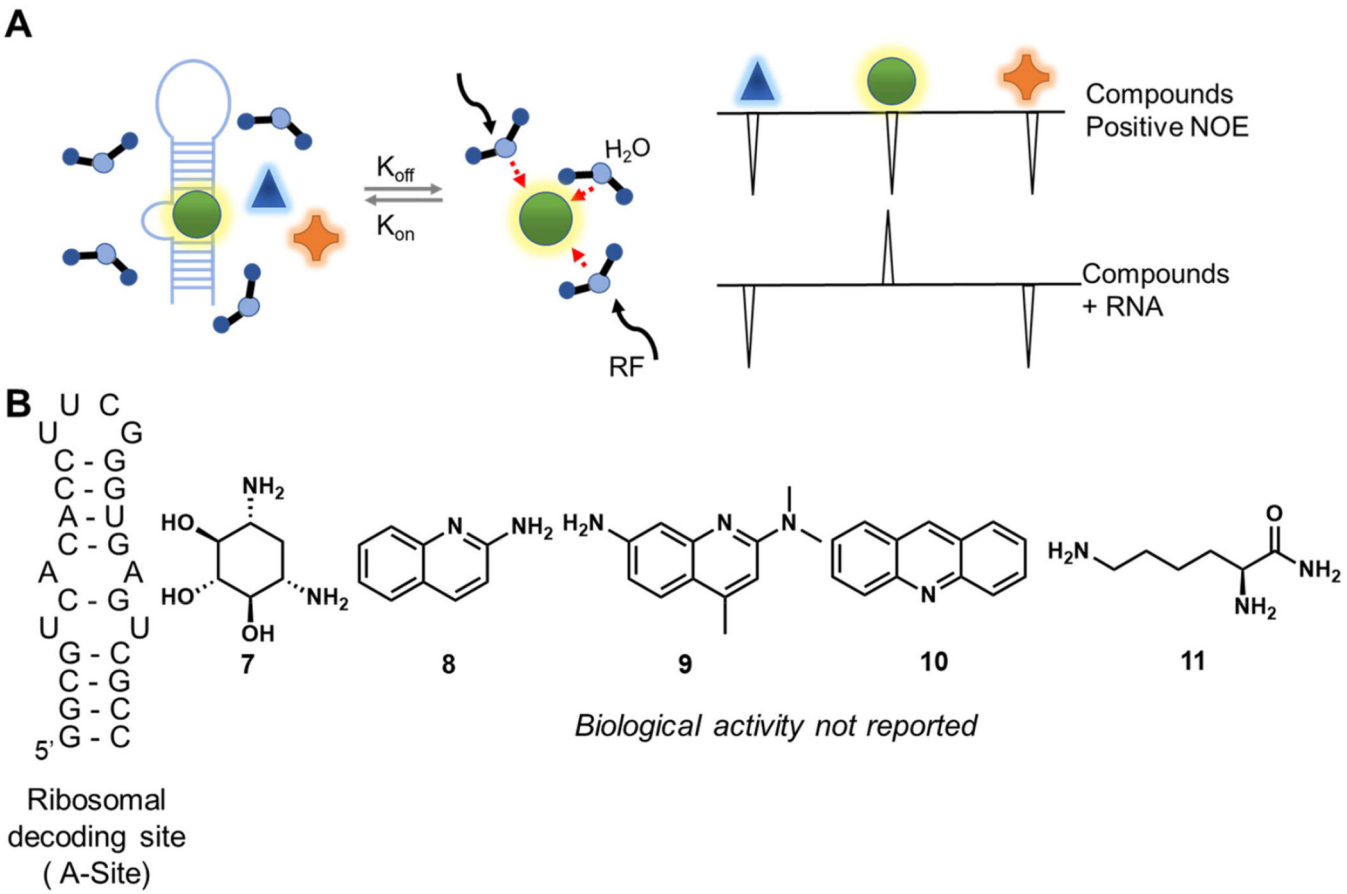

Figure 3. WaterLOGSY to identify fragments that bind RNAs.

(20) (A) Schematic for identification of fragments that bind RNA using WaterLOGSY NMR spectroscopy. Magnetization is transferred after excitation of bulk water (radiofrequency (RF) wave, black arrows). Nonbinders show positive NOEs with water. Ligands that are in fast exchange between free and bound forms; the RNA-bound ones show negative NOE, while the free ligands show positive NOEs with water. (B) Secondary structure of the ribosomal decoding A-site used in the screen and chemical structures of fragment hits.

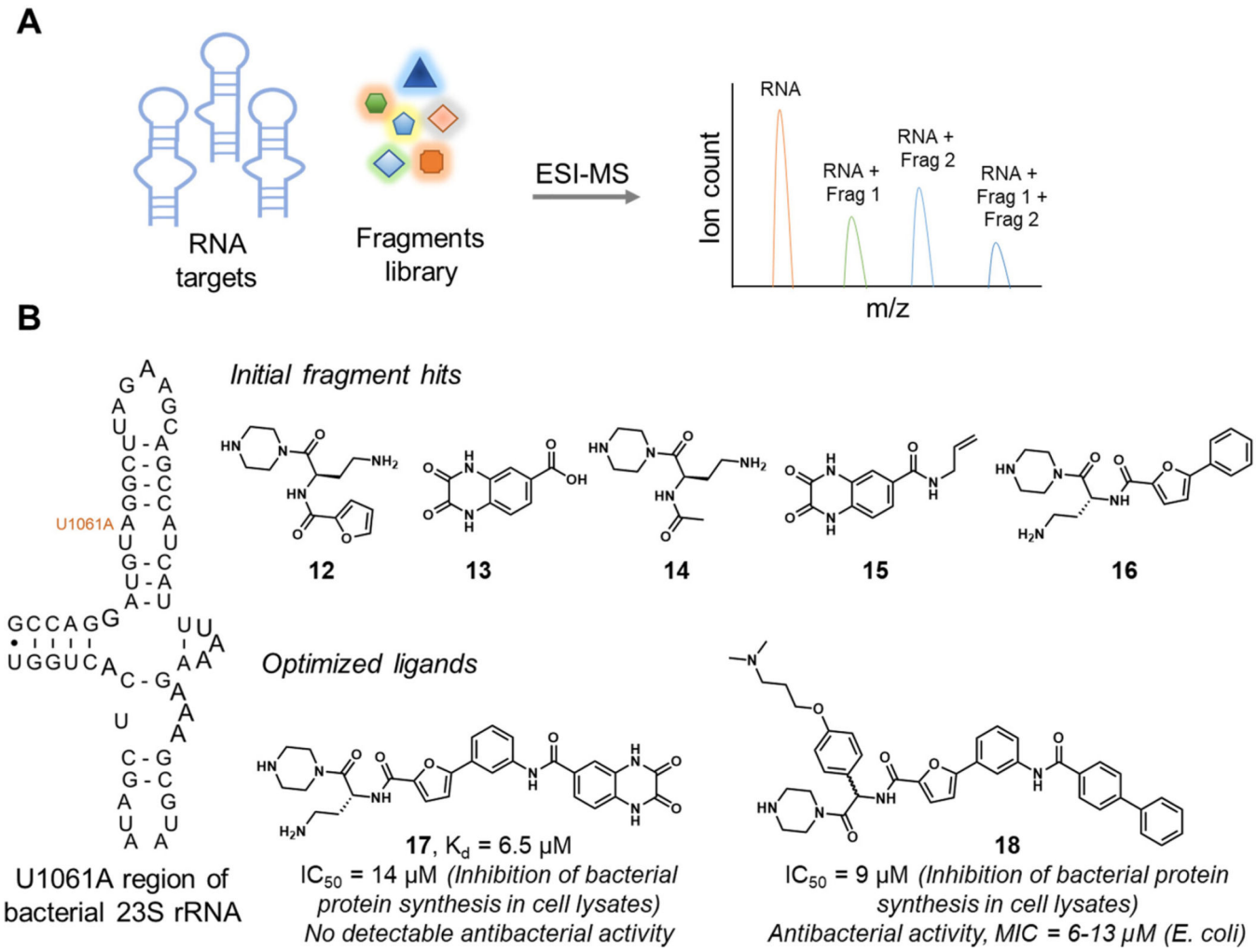

Figure 4. Mass-spectrometry-based fragment hit identification followed by optimization yielded bioactive ligands for the U1061A region of baterial 23S rRNA.

(13) (A) Schematic for identification of fragment binders to RNA using mass spectrometry. (B) Secondary structure of the U1061A region of bacterial 23S rRNA used in the screening (left) and chemical structures of fragment hits and optimized compounds (right). Optimized compound **17** inhibited protein synthesis *in vitro*; however, no antibacterial activity was detected. Optimized compound **18** demonstrates antibacterial activity with a minimum inhibitory concentration (MIC) of 6–13 μM in *E. coli*.

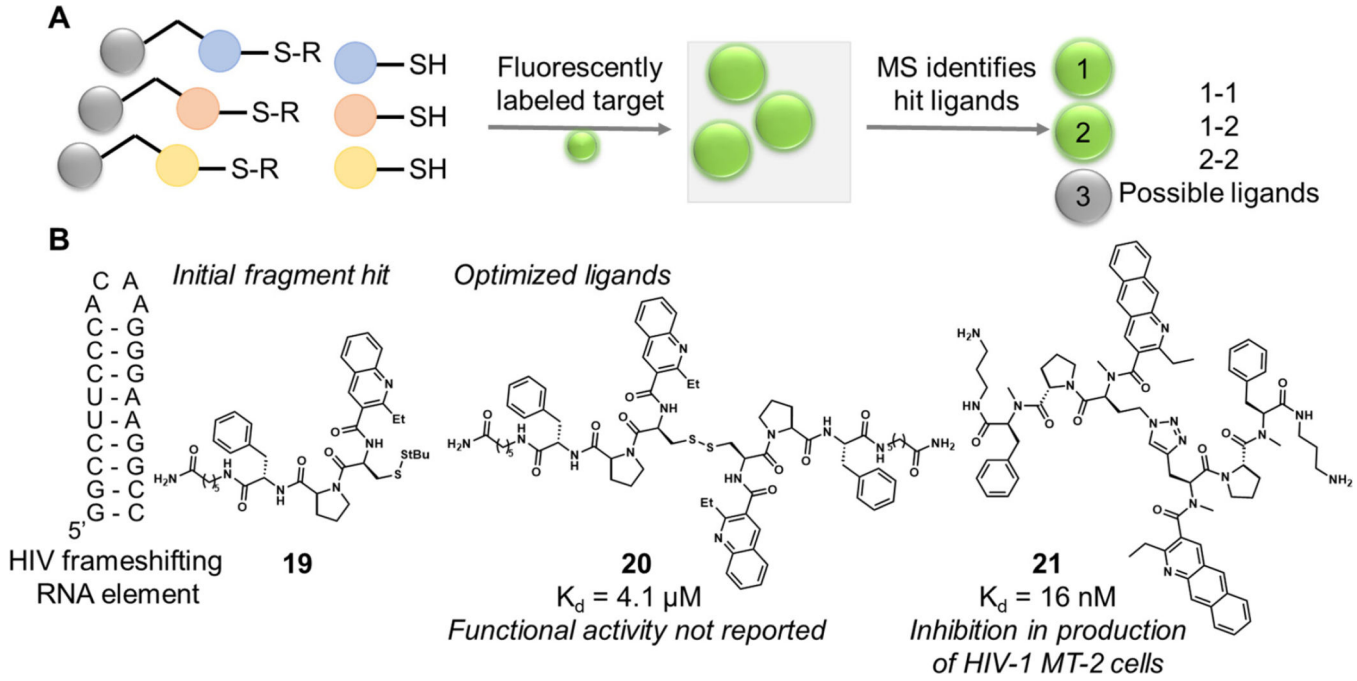

Figure 5. Dynamic combinatorial chemistry (DCC) to define building blocks that bind the HIV frameshifting element and an optimized compound that has anti-HIV activity.

(19) (A) Schematic for identification of fragment binders to RNA using dynamic combinatorial chemistry. (B) Secondary structure of the HIV frameshifting RNA element used in the screening and chemical structures of fragment hit and optimized compounds. Compound **21** inhibited the replication of HIV-1 in MT-2 cells.

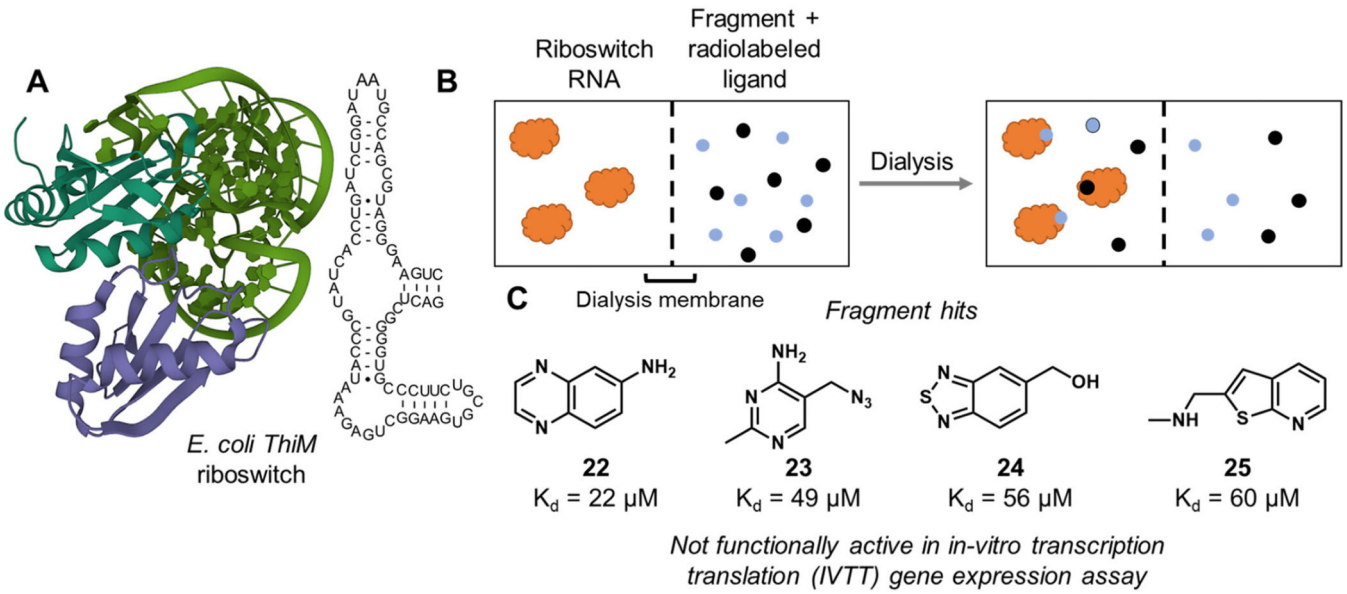

Figure 6. Equilibrium dialysis identifies fragments that bind the *E. coli ThiM* riboswitch with μM affinity.

(8) (A) Secondary structure of the *E. coli ThiM* riboswitch RNA element used in the screening. (B) Schematic for identification of fragment binders of the riboswitch using equilibrium dialysis. (C) Chemical structures of fragment hits. None of the compounds were functionally active *in vitro*, as assessed by an *in vitro* transcription translation gene expression assay.

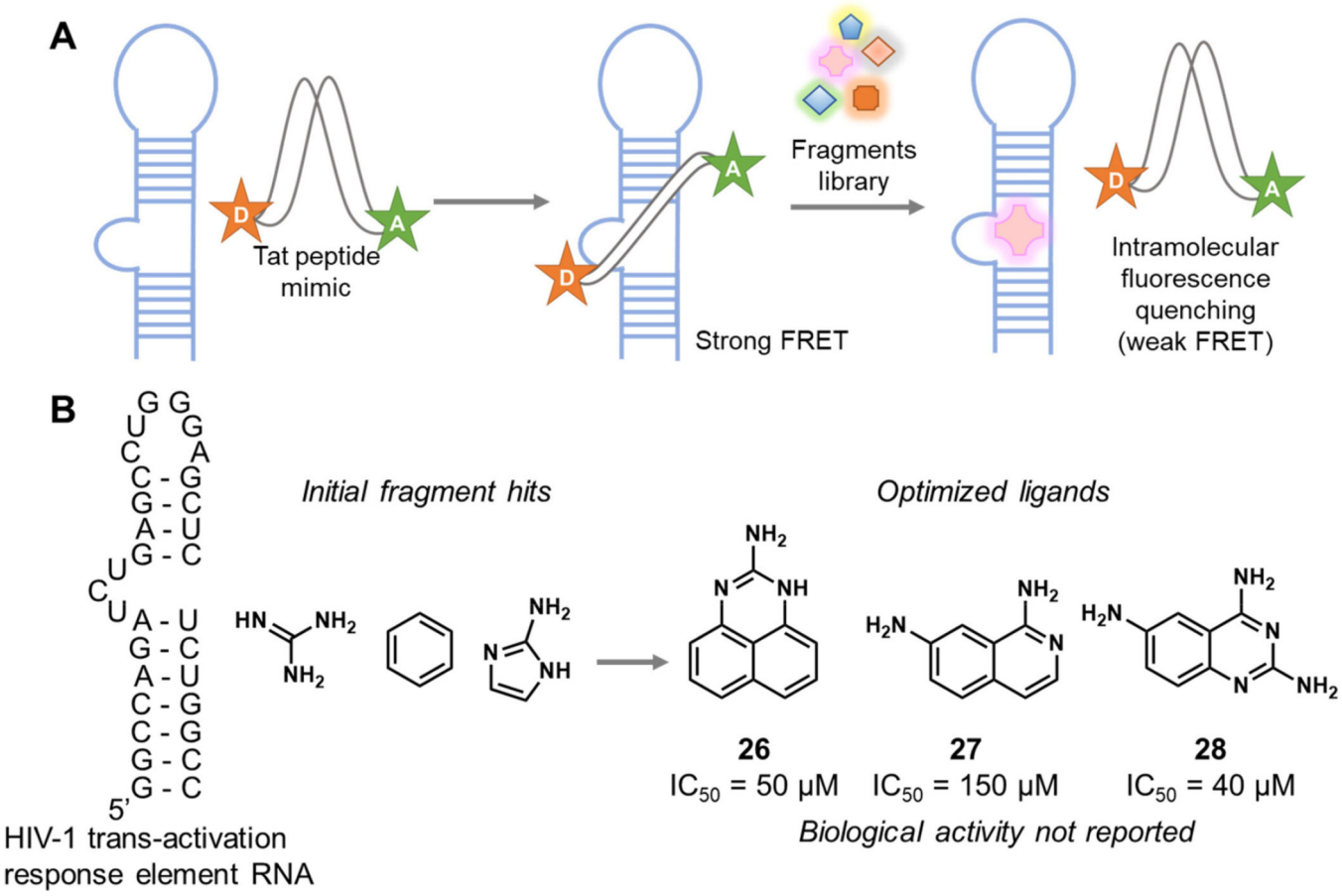

Figure 7. Fluorescent ligand displacement identifies fragment compounds that can bind HIV-1 TAR RNA with μM affinity.

(1) (A) Schematic for identification of fragment binders to RNA using fluorescent ligand displacement. (B) Secondary structure of the HIV-1 TAR RNA element used in the screening and chemical structures of fragment hits and optimized compounds. The biological activities of optimized ligands were not evaluated.

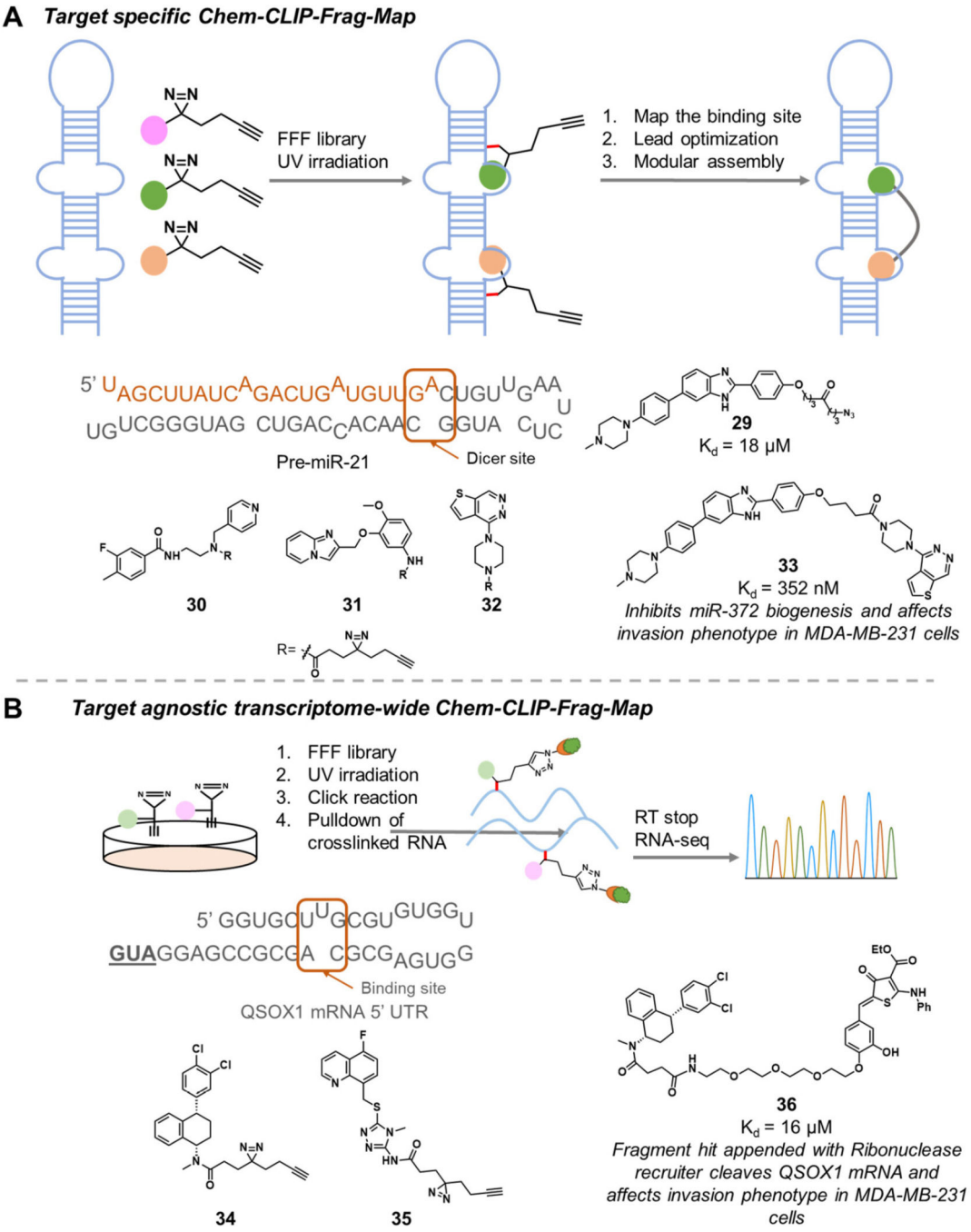

Figure 8. Chemical cross-linking and isolation by pull-down-fragment mapping (Chem-CLIP-Frag-Map) to define bioactive ligands for pre-miR-21 and *QSOX1* mRNA.

(A) Schematic for identification of fragment binders to RNA using Chem-CLIP-Frag-Map *in vitro*, the secondary structure of the pre-miR-21 RNA target, and the optimized fragment hit. (5) (B) Schematic for transcriptome-wide Chem-CLIP-Frag-Map in cells, the secondary structure of the *QSOX1* mRNA target, and the optimized fragment hit degrader. (23)

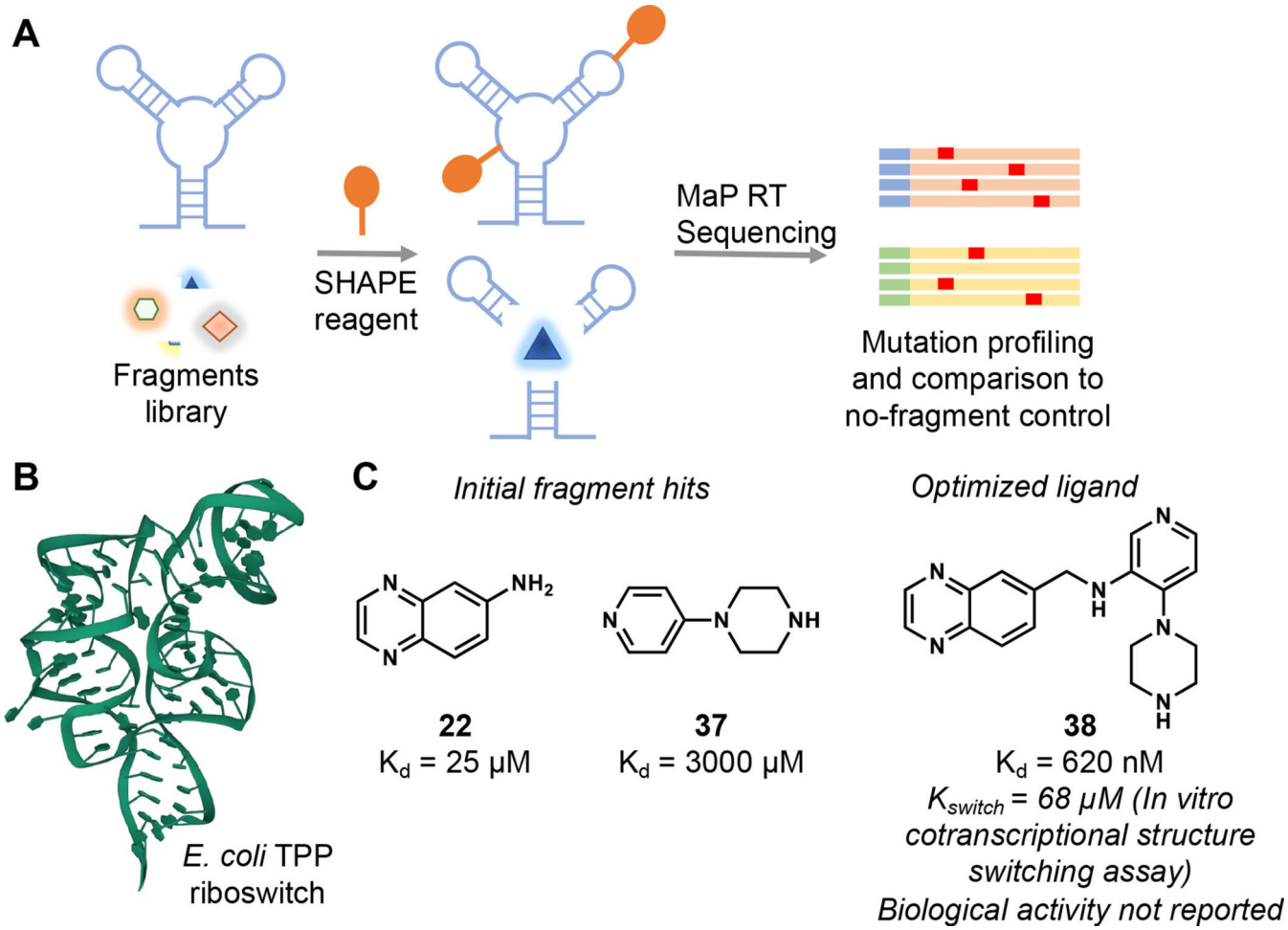

Figure 9. SHAPE-MaP defines fragments that bind the TPP riboswitch, and linking of two fragments yielded a novel ligand with increased affinity.

(2) (A) Schematic for identification of fragment binders of the *E. coli* TPP riboswitch using SHAPE-MaP. (B) Structure of the *E. coli* TPP riboswitch. (C) Chemical structures of fragment hits and optimized ligand. Compound **38** inhibited cotranscriptional structure switching *in vitro*; however, its bioactivity was not evaluated.

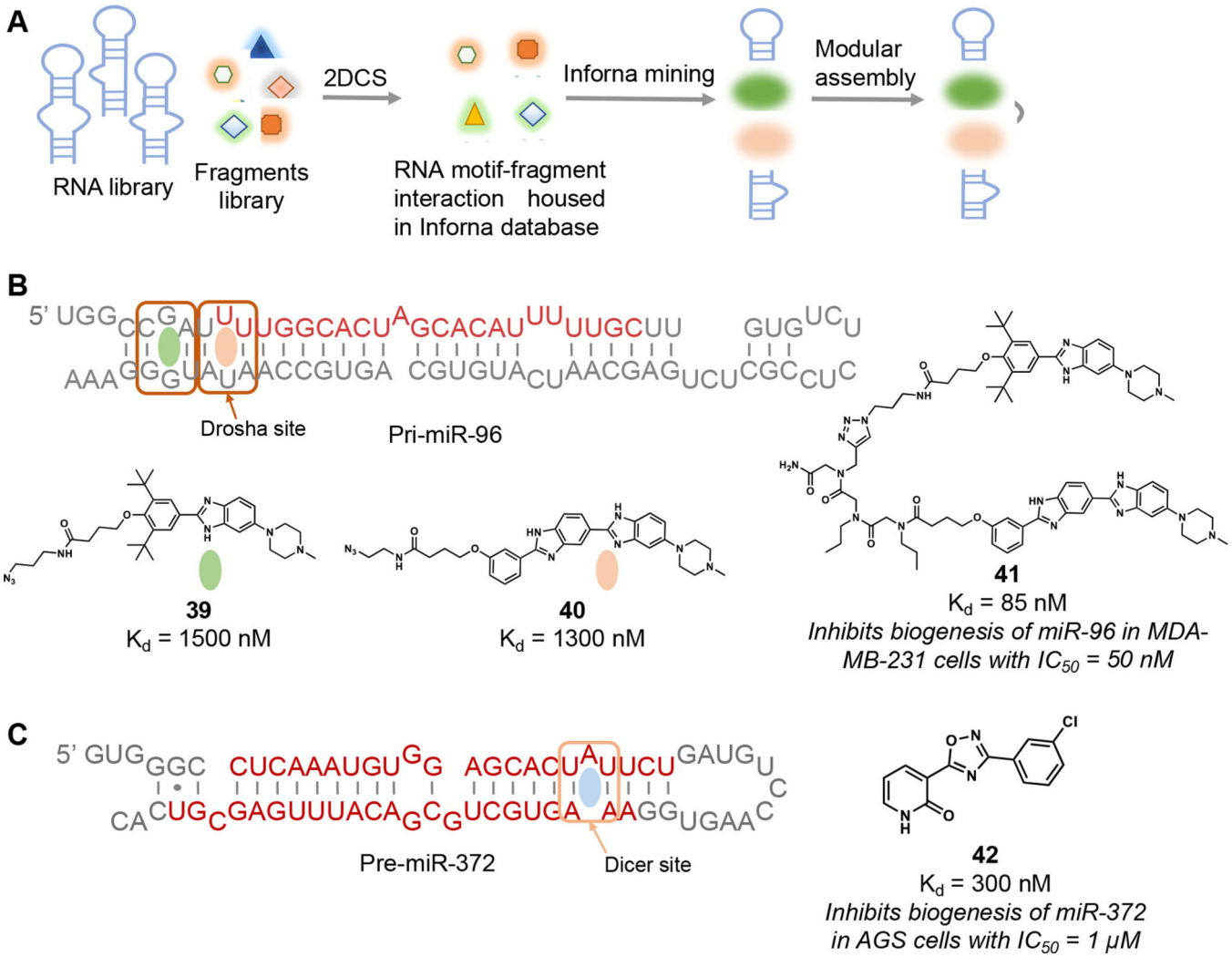

Figure 10. Sequence-based drug design using Informa and 2DCS defines ligands that bind pri-miR-96 and pre-miR-372 and optimized compounds are bioactive in disease relevant cellular systems.

(A) Schematic for identification of fragment binders to RNA using 2DCS. (B) Secondary structure of pri-miR-96 and chemical structures of small molecule hits and optimized compound. Compound **41** inhibits the biogenesis of miR-96 in MDA-MB-231 cells. (6) (C) Secondary structure of pre-miR-372 RNA and chemical structure of the fragment hit compound. Compound **42** inhibits the biogenesis of miR-372 in AGS cells. (22)

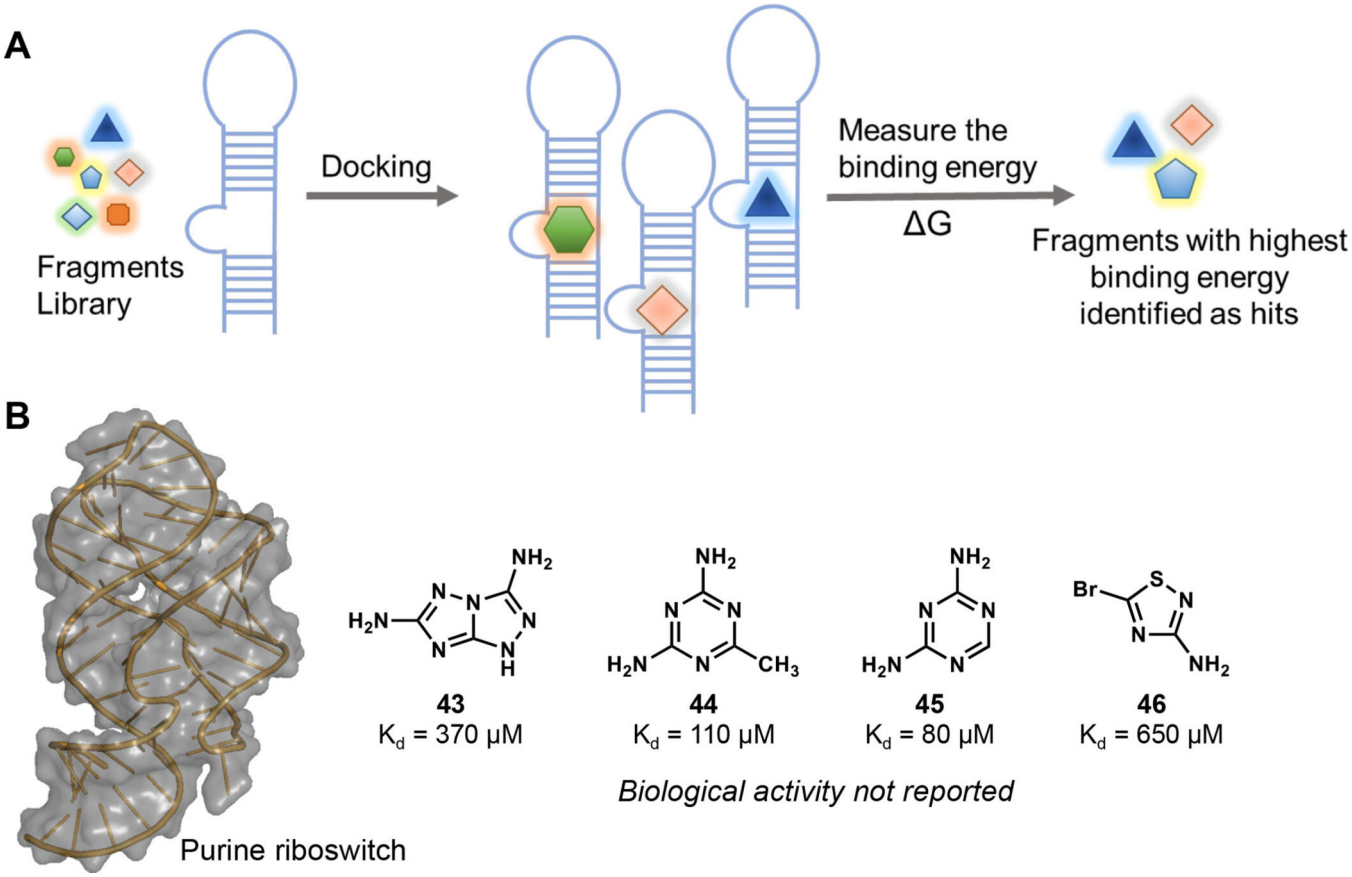

Figure 11. ***In silico*** **screening to define fragments that bind RNAs.**

(14) (A) Schematic for identification of fragment binders to RNA using virtual screening. (B) Structure of the purine riboswitch and chemical structures of fragment hits.